

MITRAC Links Mitochondrial Protein Translocation to Respiratory-Chain Assembly and Translational Regulation

David U. Mick,^{1,6,7} Sven Dennerlein,^{1,6} Heike Wiese,^{2,3} Robert Reinhold,¹ David Pacheu-Grau,¹ Isotta Lorenzi,¹ Florin Sasarman,⁴ Woranontee Weraarpachai,⁴ Eric A. Shoubridge,⁴ Bettina Warscheid,^{2,3} and Peter Rehling^{1,5,*}

¹Department for Biochemistry II, University of Göttingen, D-37073 Göttingen, Germany

²Institute for Biology II, Faculty for Biology, Functional Proteomics, University Freiburg, D-79104 Freiburg, Germany

³BIOSS Centre for Biological Signalling Studies

⁴Department of Human Genetics and Montreal Neurological Institute, McGill University, Montreal H3A 2B4, Quebec, Canada

⁵Max-Planck Institute for Biophysical Chemistry, D-37077 Göttingen, Germany

⁶These authors contributed equally to this work

⁷Present address: Department of Molecular and Cellular Physiology, Stanford University School of Medicine, Stanford, CA 94305-5345, USA

*Correspondence: peter.rehling@medizin.uni-goettingen.de

<http://dx.doi.org/10.1016/j.cell.2012.11.053>

SUMMARY

Mitochondrial respiratory-chain complexes assemble from subunits of dual genetic origin assisted by specialized assembly factors. Whereas core subunits are translated on mitochondrial ribosomes, others are imported after cytosolic translation. How imported subunits are ushered to assembly intermediates containing mitochondria-encoded subunits is unresolved. Here, we report a comprehensive dissection of early cytochrome *c* oxidase assembly intermediates containing proteins required for normal mitochondrial translation and reveal assembly factors promoting biogenesis of human respiratory-chain complexes. We find that TIM21, a subunit of the inner-membrane presequence translocase, is also present in the major assembly intermediates containing newly mitochondria-synthesized and imported respiratory-chain subunits, which we term MITRAC complexes. Human TIM21 is dispensable for protein import but required for integration of early-assembling, presequence-containing subunits into respiratory-chain intermediates. We establish an unexpected molecular link between the TIM23 transport machinery and assembly of respiratory-chain complexes that regulate mitochondrial protein synthesis in response to their assembly state.

INTRODUCTION

The mitochondrial oxidative phosphorylation system generates the bulk of cellular ATP in most eukaryotic cells. This major task of energy metabolism is fulfilled by five multisubunit protein complexes, referred to as complexes I–V, residing in the inner

membrane of mitochondria. They consist of subunits of dual genetic origin, encoded on both mitochondrial and nuclear genomes (Mick et al., 2011; Soto et al., 2012). This exceptional situation requires well-balanced and sophisticated regulation of protein expression, transport, and integration of subunits into the inner mitochondrial membrane, where they assemble to form oligomeric complexes. Cofactors, required for electron transport, have to be incorporated during the assembly process to establish functional, redox-active enzymes (Carr and Winge, 2003). At the same time, cells need to be protected from the production of deleterious reactive oxygen species formed in partially assembled complexes (Khalimonchuk et al., 2007; Shoubridge, 2001; Smeitink et al., 2006). Most of our current knowledge on human respiratory-chain biogenesis stems from analyses of patients suffering from mitochondrial encephalomyopathies, such as Leigh Syndrome.

The molecular details of the respiratory-chain assembly process are best studied for the cytochrome *c* oxidase (complex IV). Distinct steps of the assembly process have been dissected and depend on so-called assembly factors. These proteins assist in the progression of the assembly process and stabilize intermediates in the membrane. Studies in yeast have provided insight into mechanisms and regulatory principles of assembly and have identified more than 20 complex IV-specific assembly factors (Mick et al., 2011; Soto et al., 2012). Surprisingly, most of these lack robust mammalian homologs. In the course of this study, an *in silico* analysis that aimed to identify proteins with sequence similarity to these yeast factors revealed potential candidates, each of which awaits confirmation *in vivo* (Szkarczyk et al., 2012). Clearly, the highest degree of similarity is found among known factors involved in cofactor biogenesis, exemplified by the conserved SURF1/Shy1 protein, implicated in heme *a* insertion into the central subunit COX1 (Mashkevich et al., 1997). Mutations in *SURF1* are the most frequent cause of Leigh Syndrome with cytochrome *c* oxidase deficiency (Shoubridge, 2001; Smeitink et al., 2006). Interestingly, corresponding mutations in the yeast homolog Shy1 have been found to differentially

influence mitochondrial translation (Barrientos et al., 2002; Reinhold et al., 2011). In yeast, expression of mitochondria-encoded Cox1 is highly regulated at the translational level. The COX1 messenger RNA (mRNA)-specific translational activator Mss51 is recruited to and inactivated in early Cox1 assembly-intermediate complexes containing the assembly factors Cox14, Coa3, and Coa1 (Barrientos et al., 2004; Fontanesi et al., 2011; Mick et al., 2007, 2010; Perez-Martinez et al., 2003; Pierrel et al., 2007). In situations where intermediates accumulate, this complex stalls Cox1 translation, so that the Cox1 assembly status feeds back to its own translation. In human mitochondria, factors that influence COX1 translation, such as TACO1 or c12orf62 (COX14), have been described; however, it is still unclear whether they represent functional counterparts of the yeast proteins described above (Szklarczyk et al., 2012; Weraarpachai et al., 2009, 2012). Thus, molecular mechanisms that regulate COX1 translation in human mitochondria are unknown.

The assembly process of single respiratory-chain complexes revolves around membrane integration and stabilization of central mitochondria-encoded subunits that are subsequently joined by nuclear-encoded subunits entering the organelle from the cytosol. Nuclear-encoded subunits of the respiratory chain predominantly harbor N-terminal presequences for mitochondrial targeting (Vögtle et al., 2009). The molecular machines that facilitate their insertion into the mitochondrial inner membrane are well studied and highly conserved among eukaryotes (Dolezal et al., 2006). Whereas mitochondria-encoded proteins are inserted by the Oxa1 insertase, most nuclear-encoded respiratory-chain subunits are imported by the presequence translocase (TIM23 complex) (Chacinska et al., 2009; Neupert and Herrmann, 2007). This translocase consists of five membrane proteins: the channel-forming Tim23, the closely associated Tim17, the presequence receptor Tim50, Mgr2, and Tim21. Yeast Tim21 associates with respiratory-chain supercomplexes to promote insertion of presequence-containing precursors into the inner membrane (Saddar et al., 2008; van der Laan et al., 2006). This association is critical under growth conditions that restrict the membrane potential, which drives ATP synthesis and transport across the inner membrane. Despite detailed insight into the mechanism of protein import, it is still unknown how preproteins, which are inserted into the inner membrane by the presequence translocase, are directed to assembling respiratory-chain subcomplexes. So far, no assembly factors or candidate proteins that mediate transport of imported proteins to the different respiratory-chain subassemblies have been proposed.

Here, we comprehensively identified mammalian cytochrome *c* oxidase assembly factors. These analyses led to the discovery of MITRAC12, which defines the MITRAC (mitochondrial translation regulation assembly intermediate of cytochrome *c* oxidase) complexes. A detailed characterization of the MITRAC12 interaction network revealed gene products that are involved in early steps of mammalian complex IV biogenesis and link assembly to COX1 translational regulation in human. Our analyses reveal a dynamic distribution of the uncharacterized human TIM21 between TIM23 and MITRAC complexes that contain the central mitochondria-encoded subunits. We demonstrate that TIM21 is the first assembly factor that is involved in the transfer of newly

imported proteins from the presequence translocase to assembling respiratory-chain complexes.

RESULTS

MITRAC12 Associates with SURF1 and COX1 Assembly Intermediates

In human mitochondria, the molecular mechanisms and components of early steps of COX1 biogenesis are ill defined. In contrast, biochemical isolation of yeast Cox1 assembly intermediates with ZZ-tagged Shy1 as bait led to the identification of new assembly factors (Mick et al., 2007, 2010) and extended mechanistic insights into the concept of tight coupling between cytochrome *c* oxidase assembly and translational regulation of COX1 mRNA (Barrientos et al., 2004; Perez-Martinez et al., 2003). Based on this strategy, we generated a stable HEK293 cell line expressing SURF1 with a C-terminal ZZ-tag. Isolated mitochondria containing SURF1^{ZZ} were solubilized and subjected to IgG chromatography. Purified proteins were separated by SDS-PAGE (Figure 1A). Mass spectrometric analysis identified a prominent low-molecular-weight band as the uncharacterized human protein CCDC56, which we termed MITRAC12. MITRAC12 is a conserved protein with a calculated molecular weight of 11.7 kDa and contains a single predicted transmembrane span (Figure 1B). To address whether MITRAC12 was a mitochondrial protein, we synthesized and radiolabeled the protein in reticulocyte lysate. [³⁵S]MITRAC12 was subsequently imported into isolated human mitochondria, and radiolabeled ornithine-transcarbamylase (OTC) served as a control. MITRAC12 was efficiently imported into mitochondria and became protected against protease treatment. No processing of the imported protein was observed, suggesting that it is not directed into mitochondria by a cleavable presequence (Figure 1C). Although MITRAC12 import was largely dependent on the membrane potential ($\Delta\psi$) across the inner membrane, a fraction was transported into mitochondria in the absence of a $\Delta\psi$ (Figure 1C, lane 4). Similarly, $\Delta\psi$ -independent import has been reported for small inner-mitochondrial-membrane proteins (Wagner et al., 2009). To address the submitochondrial localization of MITRAC12, we generated a stable Flp-InTM T-RExTM 293 cell line expressing the protein with a C-terminal FLAG-tag under the control of a tetracycline-regulatable promoter. Similar to the inner-membrane protein TIM23, MITRAC12^{FLAG} was recovered with isolated mitochondria and only became accessible to externally added protease when the outer membrane was disrupted by hypo-osmotic treatment (mitoplasts) or sonication (Figure 1D). As MITRAC12 was resistant to carbonate extraction, we concluded that MITRAC12 was an inner-mitochondrial-membrane protein with its C terminus exposed to the intermembrane space (IMS). Identical results were obtained for authentic MITRAC12 with an antiserum directed against the C terminus (see Figure 4A). To support coisolation of MITRAC12 with SURF1, we analyzed SURF1^{ZZ} isolation samples by western blotting with an antiserum against the C terminus of MITRAC12. Whereas LETM1, an inner-mitochondrial-membrane protein, did not copurify with SURF1^{ZZ}, MITRAC12 was efficiently isolated (Figure 1E). However, only minute amounts of COX1 were coisolated, suggesting that the tagged SURF1 was functionally

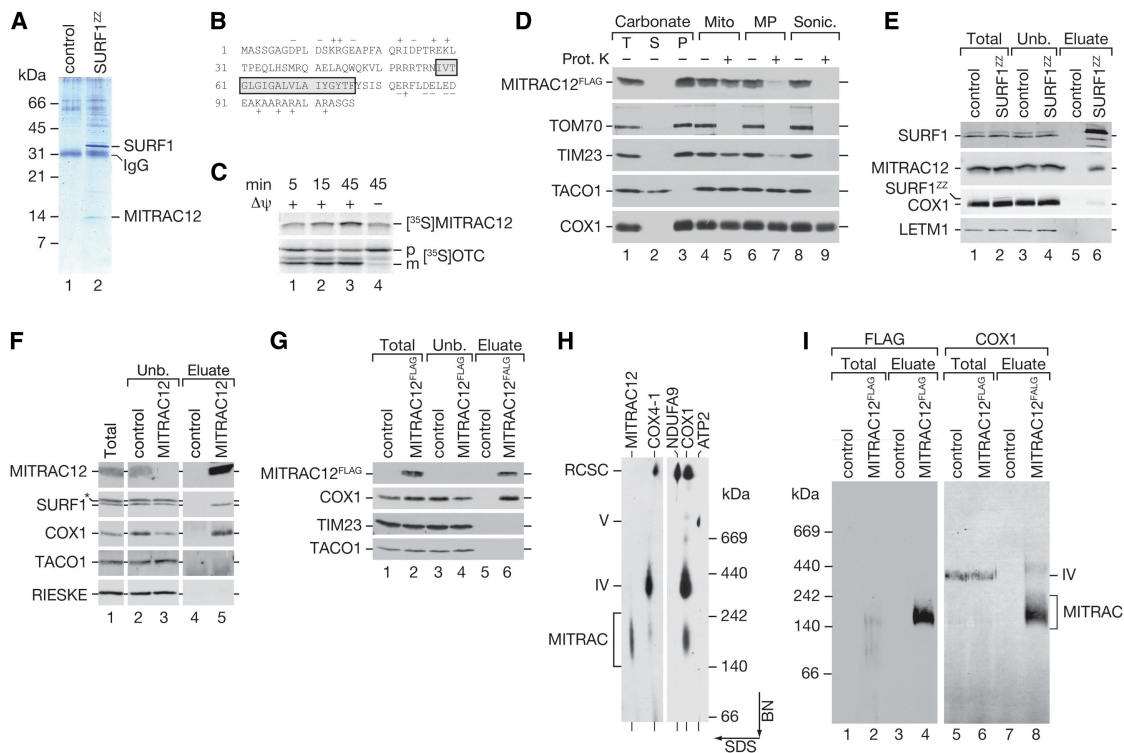


Figure 1. Identification of MITRAC12 and MITRAC Complexes

(A) Mitochondria from control and SURF1^{ZZ}-expressing HEK293 cells were solubilized and subjected to IgG chromatography. Eluates were analyzed by SDS-PAGE and LC-MS/MS.

(B) Primary structure of MITRAC12. Gray box, predicted transmembrane span.

(C) [³⁵S]MITRAC12 and [³⁵S]OTC precursors were imported into HEK293 mitochondria in the presence or absence of $\Delta\psi$, and samples were treated with proteinase K and analyzed by SDS-PAGE and digital autoradiography. p, precursor; m, mature.

(D) Membrane association and submitochondrial localization of MITRAC12^{FLAG} were analyzed as described in the [Extended Experimental Procedures](#). T, total; S, supernatant; P, pellet. Mito, mitochondria; MP, mitoplasts; Sonic., sonication; Prot. K, proteinase K.

(E) Western blot analysis of IgG chromatography as in (A).

(F) Immunoprecipitation (IP) from HEK293 cells with anti-MITRAC12 and control antisera. *, cross-reaction. Total and Unb., 7%; Eluate, 100%.

(G) IP from control or MITRAC12^{FLAG}-containing mitochondria with anti-FLAG-agarose and FLAG peptide elution. Total and Unb., 10%; Eluate, 100%.

(H) MITRAC12^{FLAG} mitochondria analyzed by 2D-BN/SDS-PAGE and western blotting with antibody mixtures (anti-MITRAC12 and anti-COX4-1; anti-NDUFA9, anti-COX1, and anti-ATP2). RCSC, respiratory-chain supercomplexes; V, complex V; IV, complex IV.

(I) IP as in (G) was analyzed by BN-PAGE.

compromised. Therefore, we immunoprecipitated authentic MITRAC12 from HEK293 cells after solubilization. Wild-type SURF1 and COX1 efficiently coprecipitated (Figure 1F), suggesting that these proteins formed a complex in the inner membrane. To address the nature of this complex under native conditions, we again utilized MITRAC12^{FLAG}, which we expressed at endogenous levels and which could be specifically eluted from an anti-FLAG antibody matrix with FLAG peptide. As for the endogenous MITRAC12, COX1 and SURF1 were specifically recovered in MITRAC12^{FLAG} immunisolations as assessed by western blotting after SDS-PAGE (Figure 1G and Figure S1A available online). When analyzing mitochondrial protein complexes by two-dimensional electrophoresis (blue native-PAGE [BN-PAGE] followed by SDS-PAGE) and western blotting, MITRAC12 comigrated with a subcomplex of COX1 that we termed MITRAC (Figure 1H). Native isolation of MITRAC12^{FLAG}-containing complexes recovered the MITRAC complex that contained COX1 (Figure 1I).

Moreover, small amounts of mature complex IV were co-isolated as indicated by the presence of a COX1-containing complex in the eluate that comigrated with mature complex IV in the total. In conclusion, purification of SURF1 led to the identification of MITRAC12, an uncharacterized human protein associated with COX1.

MITRAC12 Is Required for Efficient COX1 Translation

Copurification of MITRAC12 with COX1 and SURF1 suggested a role in early steps of cytochrome c oxidase biogenesis. Hence, we addressed whether MITRAC12 interacted with newly synthesized COX1. Therefore, we labeled mitochondrial translation products, isolated mitochondria containing MITRAC12^{FLAG}, and performed immunisolation. Purified proteins were separated by SDS-PAGE, and radiolabeled copurifying proteins were visualized by autoradiography. Among the mitochondrial translation products, COX1 was specifically

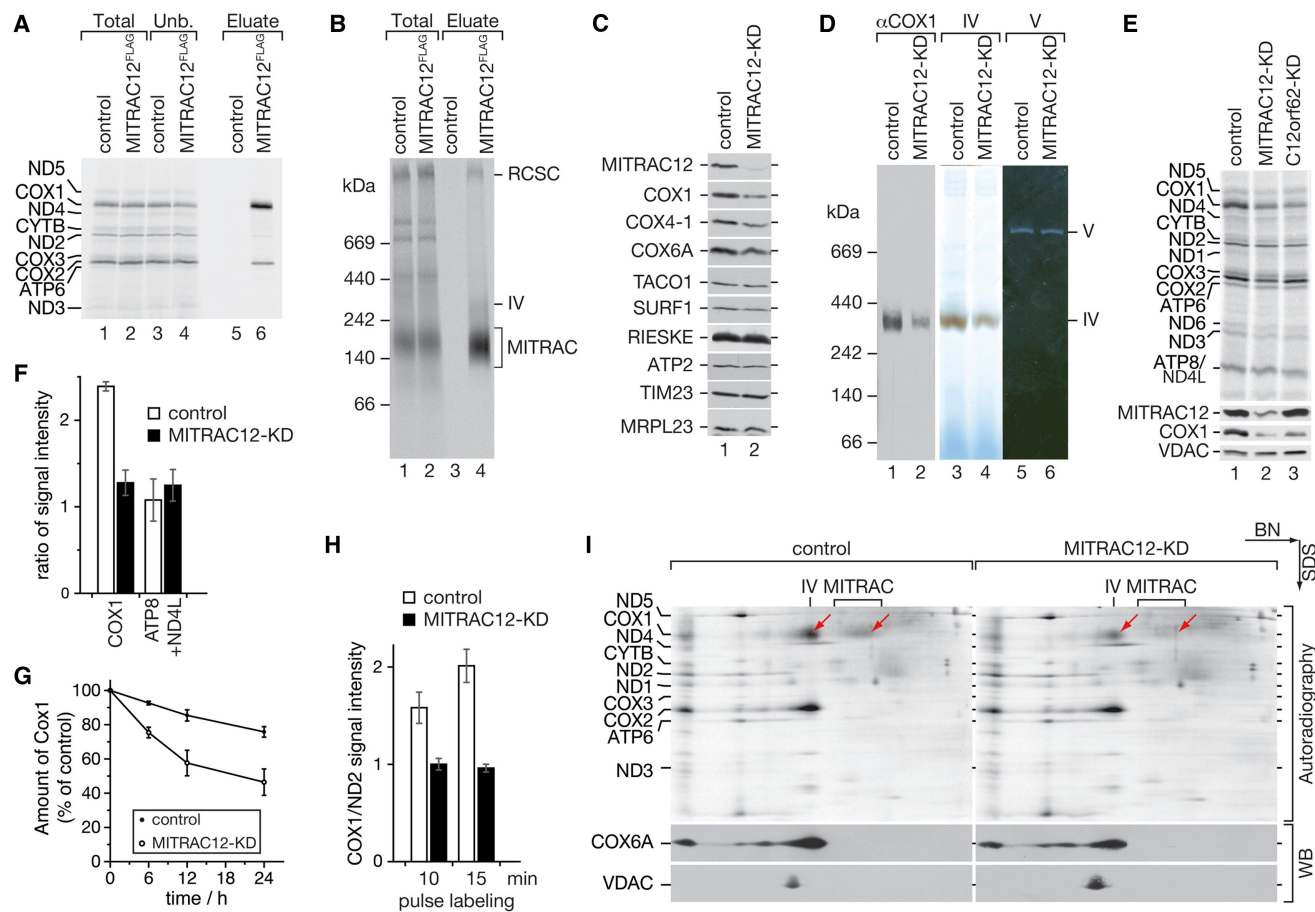


Figure 2. MITRAC12 Is a Cytochrome c Oxidase Assembly Factor Affecting COX1 Translation

(A and B) Mitochondrial translation products were labeled by [³⁵S]methionine in control and MITRAC12^{FLAG}-expressing cells for 1 hr. Anti-FLAG IP was performed as in Figure 1G. Samples were analyzed by SDS- (A) or BN-PAGE (B) and digital autoradiography. Total and Unb., 10%, Eluate, 100%. RCSC, respiratory-chain supercomplexes.

(C) Mitochondria isolated from cells treated with MITRAC12-specific or nontargeting control siRNA for 96 hr were analyzed by SDS-PAGE and western blotting.

(D) Isolated mitochondria from (C) analyzed by BN-PAGE and western blotting with COX1 antiserum or in-gel activity assays for complexes IV and V.

(E) Mitochondrial translation products were radiolabeled in HEK293 cells after siRNA treatment (72 hr) against indicated mRNAs. Cells were lysed and subjected to SDS-PAGE and autoradiography.

(F) Detected signals as in (E) were quantified and internally standardized to ND2 (SEM, n = 3).

(G) In vivo radiolabeling of mitochondrial translation products was performed for 1 hr, medium replaced, and cells further cultured in standard medium. Cells were harvested at indicated times after labeling, and proteins extracted and separated by SDS-PAGE. Ratios for COX1/COX3 signals were quantified, normalized to the pulse samples (100%), and plotted against time (SEM, n = 3); p values: 6 hr: 0.0146; 12 hr: 0.0149; 24 hr: 0.0418 (unpaired t test).

(H) Mitochondrial translation products were pulse-labeled for indicated times, and samples processed as in (E). Shown are COX1/ND2 ratios.

(I) 2D-BN/SDS-PAGE analysis of mitochondria from HEK293 cells after transfection with indicated siRNA oligos and radiolabeling of mitochondrial translation products. Upper panels, autoradiography; lower panels, western blot. Arrows indicate COX1 in mature cytochrome c oxidase and MITRAC complexes.

See also Figure S1.

enriched in the MITRAC12^{FLAG} eluate (Figure 2A). COX2 was recovered with MITRAC12 to a lesser extent, in agreement with the observed coisolation of minute amounts of mature complex IV (Figure 1I). BN-PAGE analysis of MITRAC12^{FLAG} immunoprecipitation samples after labeling of mitochondrial translation products confirmed this result and showed that no other complexes containing mitochondrial translation products were copurified (Figure 2B). To directly address whether MITRAC was a genuine COX1 assembly intermediate, we labeled mitochondrial translation products with [³⁵S]methionine and fol-

lowed the assembly of COX1 over the course of an extended chase by separating protein complexes on first-dimension BN-PAGE and subsequent second-dimension SDS-PAGE. Newly synthesized COX1 rapidly accumulated in MITRAC. Over the course of the chase, an increasing amount of radiolabeled COX1 appeared at the size of mature complex IV, while concomitantly the MITRAC signal was reduced (Figure S1B). Accordingly, COX1 was integrated into mature cytochrome c oxidase from the productive MITRAC assembly intermediate.

To analyze the function of MITRAC12 in complex IV biogenesis, we performed a small interfering RNA (siRNA)-mediated knockdown of MITRAC12 in HEK293 cells. MITRAC12 knockdown resulted in a growth defect that was rescued by expression of MITRAC12^{FLAG}, indicating that the construct was functional (Figure S1C). Specific MITRAC12 siRNA-treated and nontargeting control cells were initially subjected to steady-state protein analysis. MITRAC12-depleted cells displayed a selective reduction of COX1 and the early-assembling nuclear-encoded subunit COX4-1. In contrast, COX6A, a peripheral late-assembling complex subunit, was hardly affected (Figure 2C). In agreement with this observation, mitochondria from MITRAC12-depleted cells displayed reduced cytochrome c oxidase activity as assessed by in-gel activity staining of mitochondrial protein complexes and enzyme activity measurements, whereas complex V activity was not affected (Figures 2D and S1D). When we analyzed the amounts of complex IV by BN-PAGE and western blotting or ELISA, we found them significantly reduced in mitochondria lacking MITRAC12 as compared to the control (Figures 2D and S1E). The loss of cytochrome c oxidase activity in MITRAC12 siRNA-treated cells directly correlated with the reduction in the amount of complex IV, suggesting that the remaining complexes maintained wild-type activity (Figure S1F). Because MITRAC12 had not been identified as a complex IV subunit, we reasoned that MITRAC12 could be involved in complex IV biogenesis. Yeast complex IV assembly mutants and patient cells affected in c12orf62 display defects in COX1 translation. Thus, we used metabolic labeling to analyze mitochondrial translation in cells depleted for MITRAC12 or c12orf62. COX1 translation was specifically affected in HEK293 cells with reduced levels of MITRAC12 or c12orf62 (Figure 2E). Similarly, the selective reduction of COX1 was also apparent when fibroblasts were used (Figure S1G). COX1 labeling was reduced to approximately 50% (Figure 2F). To address whether the reduction of COX1 in MITRAC12-depleted cells was due to increased turnover by the mitochondrial quality-control system, we pulse-labeled mitochondrial translation products in control and MITRAC12-depleted cells and followed the labeled proteins for prolonged time. The stability of COX1 was clearly reduced in MITRAC12-depleted cells compared to control cells after extended chase periods; however, the half-life of COX1 in MITRAC12-depleted cells exceeded 21 hr (Figure 2G). To ascertain that the reduction of the COX1 signal primarily reflected a reduced rate of translation, we used pulse-labeling to analyze the synthesis of mitochondrial translation products at short time points of 10 and 15 min. As expected, COX1 synthesis was specifically reduced in MITRAC12-depleted cells (Figure 2H). The level of COX1 synthesis and partial stability upon MITRAC12 depletion is probably due to residual amounts of MITRAC12 still present in mitochondria (see Figures 2C and 2E).

To address whether the observed reduction in COX1 translation correlated with a lack of MITRAC, labeled mitochondria-encoded proteins that assembled into mitochondrial protein complexes were analyzed by 2D-BN/SDS-PAGE. These analyses revealed a specific reduction of COX1 in the MITRAC complex and concomitantly a reduction of newly synthesized COX1 in mature cytochrome c oxidase (Figure 2I). Based on

these findings, we concluded that MITRAC12 was involved in early steps of COX1 assembly, manifested in the MITRAC complex. Moreover, our experiments reveal a specific role of MITRAC12 in COX1 translation, indicating a tight coupling between complex assembly and the translational regulation of its core subunit, as seen in yeast.

MITRAC12 Interacts with Multiple Assembly Factors

To define interactions of MITRAC12, we used a quantitative affinity purification/mass spectrometry (AP/MS) approach. MITRAC12-containing complexes were purified via MITRAC12^{FLAG} after differential stable isotope labeling with amino acids in cell culture (SILAC). A fraction of the eluates was analyzed by western blotting for the presence of MITRAC12, COX1, and SURF1 (Figure 3A). Remaining eluates were analyzed by SDS-PAGE separation and quantitative MS to determine proteins that were specifically enriched with the bait (see Experimental Procedures). Four independent replicates were performed, and the mean ratios of proteins quantified in at least two replicates were plotted against their p values (Figure 3B and Table S1). Among the specific MITRAC12 interaction partners were central structural complex IV subunits such as COX1, COX3, COX4, COX5A, and COX6C and the assembly factors SURF1, COX15, COX16, as well as the recently identified c12orf62. Unexpectedly, we identified an uncharacterized protein resembling the TIM23 complex subunit Tim21 in yeast as an interacting protein. Moreover, the uncharacterized open reading frame c7orf44, the protein product of which has sequence similarity to yeast Coa1 (Szklarczyk et al., 2012) and that we term MITRAC15, as well as CMC1, a protein that is suggested to play a role in copper trafficking in yeast (Horn et al., 2008), were identified. Western blot analyses confirmed interactions with TIM21, COX subunits, SURF1, c12orf62, and MITRAC15, whereas abundant proteins of other complexes were not copurified with MITRAC12 complexes (Figure 3C).

Because c12orf62 was recently identified as a protein required for complex IV biogenesis and shown to be involved in regulation of COX1 translation, we set out to address whether COX1, MITRAC12, and c12orf62 formed a common complex. Therefore, a stable cell line expressing c12orf62^{FLAG} was generated, and complexes containing the FLAG-tagged protein were isolated. Similar to MITRAC12^{FLAG}, c12orf62^{FLAG} efficiently coisolated COX1 and SURF1 (Figure 3D). Moreover, BN-PAGE analyses confirmed the presence of MITRAC12 and COX1 in an isolated complex resembling MITRAC (Figure 3E). Considering the previously identified role of c12orf62 in COX1 translation and the fact that a loss of its function leads to cytochrome c oxidase deficiency, causing fatal neonatal lactic acidosis (Weraarpachai et al., 2012), its identification as a MITRAC constituent supports our experimental strategy to identify assembly factors. Moreover, we hypothesize that proteins identified here could represent candidates affected in human oxidative phosphorylation disorders.

MITRAC15 and CMC1 Display Different Interaction Patterns

One disease-candidate protein, MITRAC15, was uncharacterized and previously not linked to mitochondrial function. Thus,

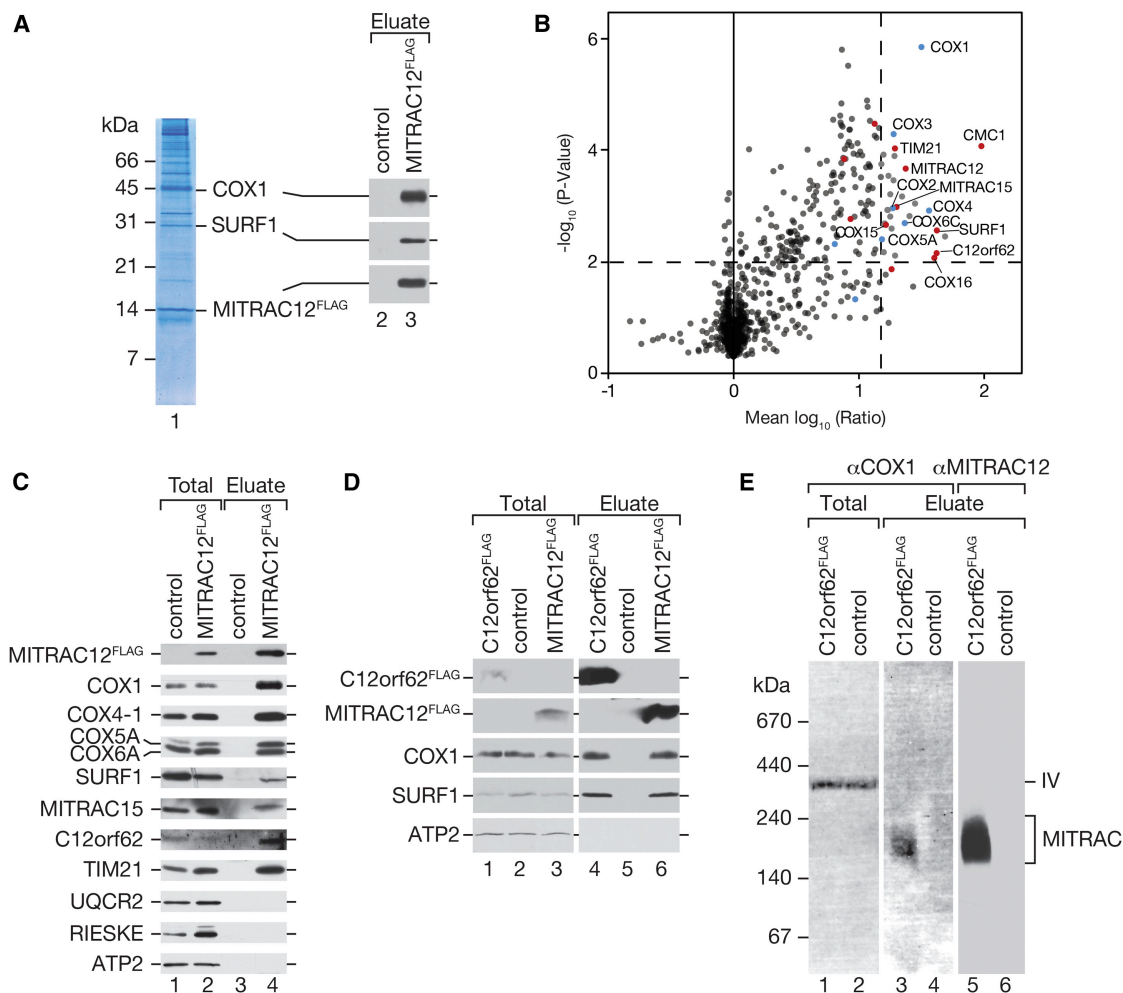


Figure 3. MITRAC12 Interaction Network Reveals Interaction with c12orf62

(A) SILAC to differentially label MITRAC12^{FLAG}-expressing and control cells. Equal amounts of mitochondria were solubilized and subjected to anti-FLAG IP followed by native elution. Eluate was analyzed by SDS-PAGE and LC-MS or western blotting.

(B) Normalized enrichment ratios were calculated from four independent experiments with label switch as in (A) and log-transformed. Mean enrichment ratios were plotted against p values determined by a one-sided t test. Significance thresholds were set at p values < 0.01 and mean enrichment ratios > 15 (dashed lines). Structural complex IV subunits: blue; known and novel assembly factors: red.

(C–E) Anti-FLAG IPs from indicated cell lines, analyzed by SDS- (C and D) or BN-PAGE (E), followed by western blotting. Total, 3.3%, Eluate, 100%. See also Table S1.

we generated a MITRAC15^{FLAG}-expressing cell line to analyze protein interactions and its submitochondrial localization and topology. Like other integral membrane proteins, such as TIM23 or MITRAC12, MITRAC15 was recovered in the pellet fraction after carbonate extraction and ultracentrifugation (Figure 4A). Moreover, the C-terminal FLAG-tag was protected from externally added protease in intact mitochondria and only became accessible when the outer membrane was ruptured by osmotic swelling or membrane solubilization, whereas the mitochondrial inner-membrane protein LETM1 that faces the matrix remained protected in mitoplasts (Figure 4A, lanes 4–9). Thus, MITRAC15 behaved as an integral membrane protein with its C terminus facing the IMS. Immunoprecipitation of MITRAC15^{FLAG} led to coprecipitation of MITRAC12, SURF1, COX1, and TIM21, supporting the

observed coisolation analyses. Surprisingly, we reproducibly coisolated the integral membrane protein NDUFB8, a subunit of complex I, with MITRAC15, whereas tested subunits of complexes III and V were not recovered (Figure 4B). Despite this association, the FLAG-tagged MITRAC15 could not be detected in complexes on BN-PAGE (data not shown). It is possible that the C-terminal tag in combination with the harsh BN-PAGE conditions, in which the Coomassie dye can affect the stringency of detergent properties (Wittig et al., 2006), dissociated it from complexes. To assess the role of MITRAC15 in respiratory-chain biogenesis, we analyzed MITRAC15 knockdown cells by BN-PAGE. In knockdown cells, the levels of cytochrome c oxidase and NADH CoQ reductase (complex I) were specifically affected (Figure 4C). As a loading control, we decorated complexes II, III,

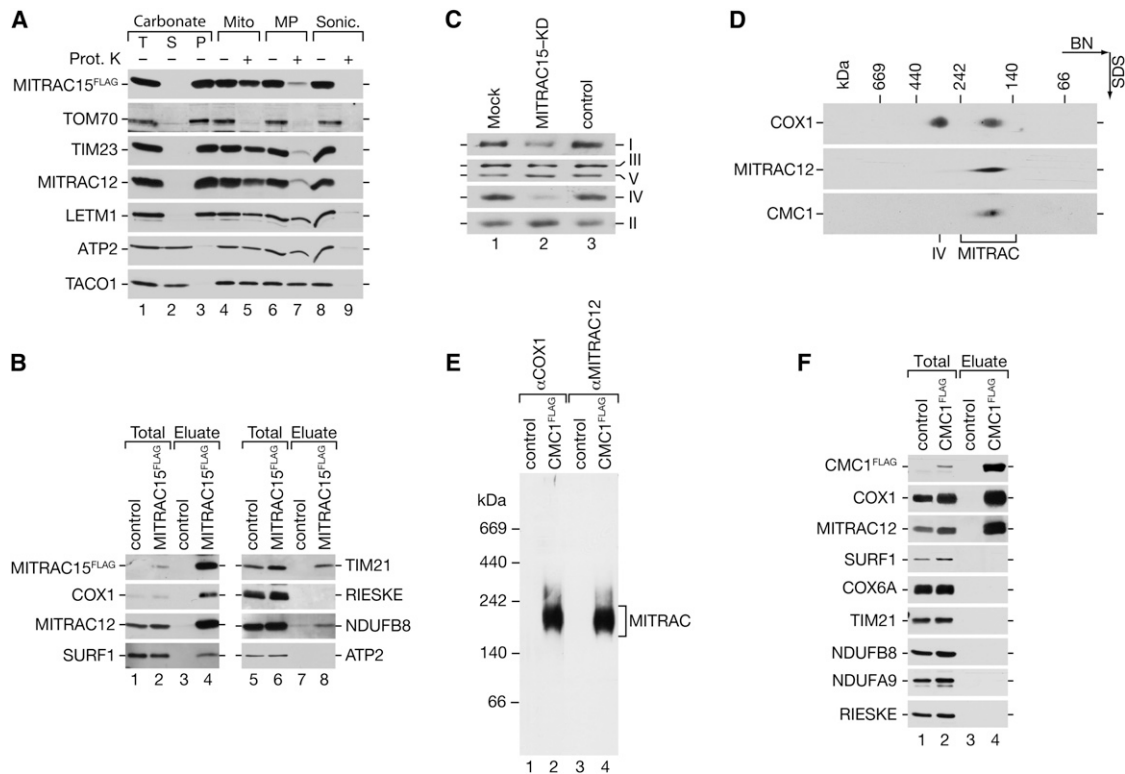


Figure 4. MITRAC15 and CMC1 Are MITRAC-Associated Assembly Factors

(A) Membrane association and submitochondrial localization of MITRAC15^{FLAG} as described in the [Extended Experimental Procedures](#). T, total; S, supernatant; P, pellet; Mito, mitochondria; MP, mitoplasts; Sonic., sonication; Prot. K, proteinase K. (B) MITRAC15^{FLAG} mitochondria were solubilized, and IPs performed with anti-FLAG-agarose. Samples were analyzed by SDS-PAGE and western blotting. (C) BN-PAGE analysis of indicated siRNA knockdown fibroblasts. Antibodies directed against subunits of OXPHOS complexes I–V were used for immunoblotting. (D) Isolated mitochondria containing CMC1^{FLAG} and analyzed by 2D-BN/SDS-PAGE and western blotting. (E and F) Anti-FLAG IP from solubilized CMC1^{FLAG} mitochondria analyzed by BN- (E) or SDS-PAGE (F) and western blotting. Total, 1%; Eluate, 50% for SDS-PAGE, 100% BN-PAGE.

and V, the levels of which were reproducibly not significantly affected upon MITRAC15 depletion. A quantification of complex IV and I levels revealed an 80% and 40% reduction, respectively. Hence, we concluded that MITRAC15 functions in both complex IV and complex I biogenesis.

Next, we analyzed CMC1 complexes in mitochondria from a stable cell line expressing CMC1^{FLAG}. In 2D-BN/SDS-PAGE analyses, CMC1 formed complexes that comigrated with the MITRAC complex (Figure 4D). To show that these complexes represented the identical species rather than comigrating independent complexes, we performed anti-FLAG purification. CMC1 efficiently isolated solely the MITRAC complex on BN-PAGE (Figure 4E), which could be confirmed by SDS-PAGE analysis. However, in contrast to MITRAC15^{FLAG}, CMC1^{FLAG} did not coisolate SURF1 or TIM21 in significant amounts, suggesting that the MITRAC complex detected on BN-PAGE represented a heterogeneous population (Figure 4F).

By analyzing MITRAC12 interaction partners, we show that recently identified assembly factors, such as c12orf62, CMC1, and the novel assembly factor MITRAC15, are constituents of MITRAC complexes. Moreover, our analyses link MITRAC15 to both complex I and IV biogenesis.

TIM21 Is a Constituent of Cytochrome c Oxidase Assembly Intermediates

To evaluate MITRAC12-containing complexes in an unbiased approach, we performed quantitative MS analyses of protein complexes after separation by BN-PAGE. We carried out SILAC and isolated MITRAC12^{FLAG}-containing complexes from differentially labeled mitochondria for subsequent separation by BN-PAGE. A fraction of the eluates were analyzed by western blotting, revealing specific enrichment of MITRAC complexes (Figure 5A). The majority of the sample was applied to a single gel lane, stained with colloidal Coomassie, and cut into 20 slices for liquid chromatography-mass spectrometry (LC-MS) analyses. After quantification, the normalized abundance profiles of the identified proteins were calculated (Table S2). The MITRAC12 (bait) profile displayed several peaks of different intensities (Figure 5B, left). Slices 18–20 corresponded to the bottom of the BN-PAGE lane, where monomeric proteins not in complex with other proteins would be expected. The small peak in fraction 10 corresponded in size to mature complex IV. Indeed, except for COX1, all identified cytochrome c oxidase structural subunits showed the highest abundance in slice 10 (Figure 5C). MITRAC12, however, exhibited highest abundances in two additional peaks (slices 13 and 15)

that correspond in size to the MITRAC complexes. Consistently, the COX1 profile displayed several distinct intensity maxima in slices 10, 13, and 15. Moreover, other MITRAC components, such as CMC1 and c12orf62, peaked in slice 15. For an unbiased classification of the identified proteins into different complexes, the profiles calculated based on two independent experiments (including label-switch) were subjected to hierarchical clustering. These analyses resulted in five clusters, the mature cytochrome c oxidase (cluster 3), the MITRAC complexes (cluster 2), and three clusters comprising protein profiles that did not overlap with any of the MITRAC12 peaks that were grouped and displayed in a heatmap (Figure 5B and Table S2). Components of these three clusters, such as the highly abundant mitochondrial ATP-Synthase (cluster 1) and hydrophobic carrier proteins (cluster 4), represent prominent contaminations of native complex isolations with the mild detergent digitonin. Cluster 5 identified proteins that peaked in fractions 1 or 2, indicating that these did not run into the gel and therefore could represent aggregates.

Interestingly, the protein profiles of the cytochrome c oxidase subunits that assemble early with COX1, such as COX4, COX6C, and COX5A, showed a discrete shoulder in fractions 12 and 13, which was not observed for other subunits. TIM21 also showed highest intensities in the same fractions (Figure 5C). This distribution indicated that the TIM21-containing assembly intermediate containing COX1 represented a subpopulation of MITRAC complexes. Indeed, after isolation of MITRAC12-containing complexes, 2D-BN/SDS-PAGE revealed several COX1 complexes, whereas only one complex corresponded in size to that of TIM21 (Figure 5D).

In yeast, Tim21 is part of the TIM23 complex that integrates presequence-containing proteins into the inner mitochondrial membrane. To analyze whether human TIM21 was also part of the translocase, we generated cell lines expressing FLAG-tagged TIM21 or TIM23 under regulatable promoters and isolated interacting proteins via anti-FLAG chromatography. When complexes were isolated via TIM23^{FLAG}, western blot analyses confirmed the association of TIM21 with the presequence translocase (Figure 5E), whereas complex IV assembly factors were not recovered (Figure S2A). On the other hand, isolation of TIM21^{FLAG}-containing complexes efficiently coisolated not only the presequence translocase (see Figure 6D) but also MITRAC12 and MITRAC15 (Figure 5F). However, SURF1 did not copurify with TIM21^{FLAG}. These results support the idea that TIM21 not only is part of the presequence translocase but additionally associates with a subset of complex IV assembly factors.

TIM21 Is an Assembly Factor for Respiratory-Chain Complexes

The presence of TIM21 in both the TIM23 complex and cytochrome c oxidase assembly intermediates led us to address TIM21's function in human mitochondria. siRNA-mediated knockdown of TIM21 resulted in a severe growth reduction in HEK293 cells that was rescued upon expression of siRNA-resistant TIM21^{FLAG} (Figure 6A). To test whether the observed growth defect was due to reduced import efficiency, we performed *in vitro* import into TIM21-depleted mitochondria. The presequence translocase substrate OTC was efficiently imported into control and TIM21-depleted mitochondria (Figure 6B). In

contrast, mitochondria isolated from cells depleted of TIM23 showed a drastic OTC import defect (Figure 6C). Therefore, we concluded that the observed growth defect of cells lacking TIM21 was not due to defects in protein import.

To verify a TIM21 function in complex IV assembly, we immunoprecipitated TIM21^{FLAG}-containing complexes. Besides complex IV assembly factors (MITRAC12), COX1 and the early-assembling membrane protein COX4-1 were specifically coisolated (Figure 6D). In contrast, the late-assembling membrane protein COX6A or tested subunits of complexes III and V were not recovered, indicating that respiratory-chain supercomplexes did not copurify (Figure 6D). In yeast, Tim21 associates with respiratory-chain supercomplexes formed by complexes III and IV (Saddar et al., 2008; van der Laan et al., 2006). To confirm that human TIM21 did not associate with supercomplexes but was rather present in a subset of assembly intermediates, we used FLAG-tagged COX6C and COX6A, subunits that assemble early and late into complex IV, respectively (Lazarou et al., 2009; Mick et al., 2007; Strogolova et al., 2012; Vukotic et al., 2012). Native isolation of COX6C^{FLAG} efficiently enriched respiratory-chain supercomplexes, represented by COX1, COX5A, and COX6A, as well as RIESKE and NDUF8 (Figure 6E). Moreover, the assembly factors MITRAC12 and SURF1 were enriched, along with TIM21. On the contrary, no TIM21 but only complex IV structural subunits and respiratory-chain supercomplexes (indicated by the presence of the complex I matrix-arm protein NDUF9) copurified with the late-assembling subunit COX6A^{FLAG} (Figure 6F), suggesting that human TIM21 does not associate with mature cytochrome c oxidase complexes but rather represents a constituent of assembly intermediates.

TIM21 Is Required for Assembly of Imported Complex IV Subunits

Because TIM21 interacted with MITRAC complexes, we analyzed whether TIM21 also associated with newly synthesized mitochondria-encoded respiratory-chain subunits. Therefore, we radiolabeled mitochondrial translation products in cells expressing MITRAC12^{FLAG}, TIM21^{FLAG}, or TIM23^{FLAG} and immunoprecipitated FLAG-containing complexes. Purified proteins were separated by SDS-PAGE and visualized by autoradiography (Figure 7A). TIM21^{FLAG} interacted with a number of newly synthesized mitochondrial translation products, namely COX1, COX2, and COX3 of complex IV, CYTB of complex III, and ND2, ND4, and ND5 of complex I. In contrast, MITRAC12^{FLAG} enriched mainly cytochrome c oxidase subunits, predominantly COX1, whereas TIM23^{FLAG} showed only background association. As assembly intermediates of mitochondria-encoded complex I subunits can be visualized by BN-PAGE (Dunning et al., 2007), we isolated MITRAC12^{FLAG}, TIM21^{FLAG}, or TIM23^{FLAG} complexes under native conditions after labeling of mitochondrial translation products. All proteins were efficiently isolated, and MITRAC12 and TIM21 copurified expected amounts of COX1 (Figure 7B). When eluates were analyzed by BN-PAGE and autoradiography, TIM21^{FLAG} enriched several protein complexes of different sizes (Figure 7C). One TIM21^{FLAG}-isolated complex of around 180 kDa appeared to comigrate only with the slower-migrating cytochrome c oxidase assembly-intermediate species, consistent with our 2D-PAGE analysis of isolated

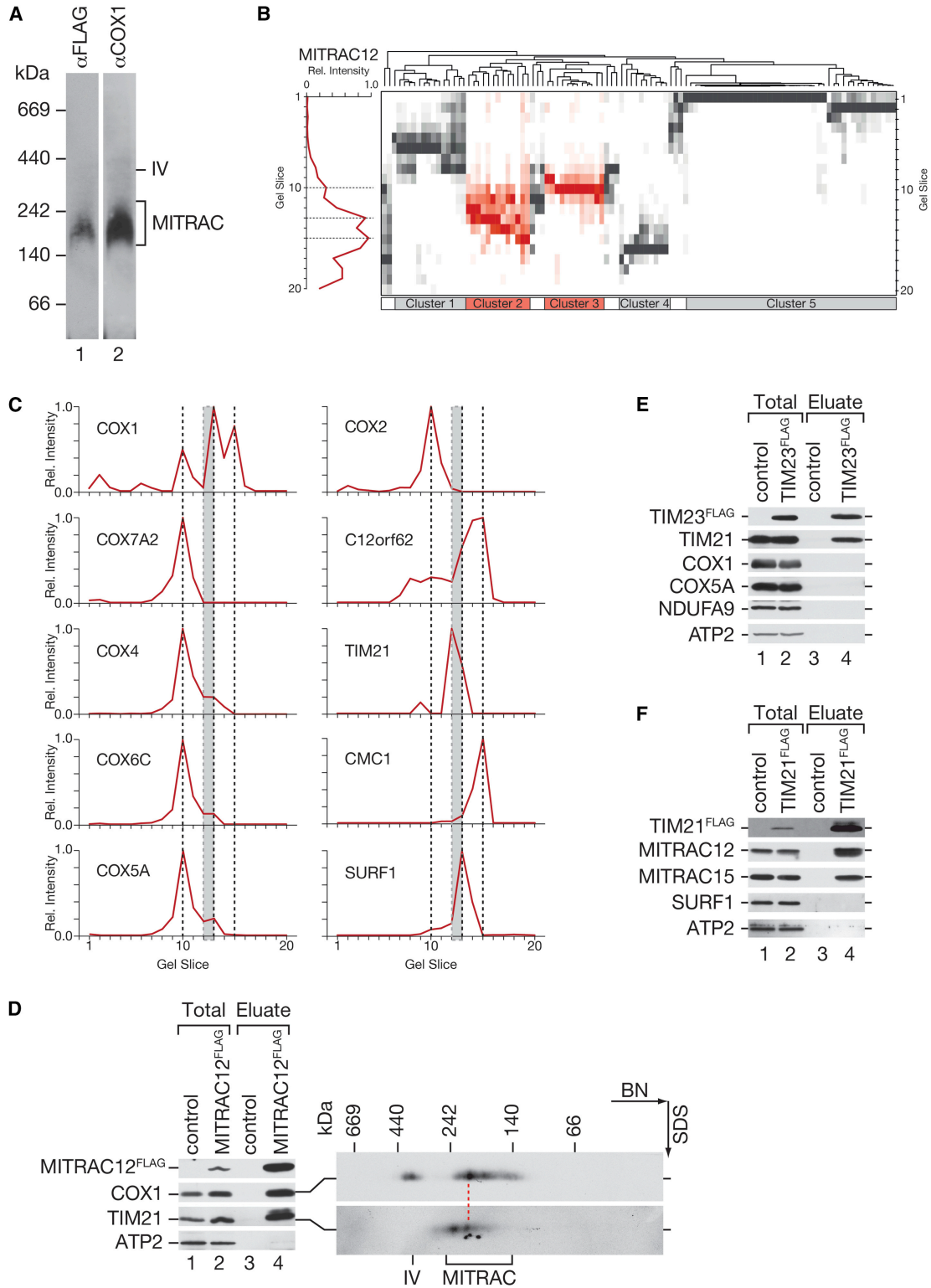


Figure 5. TIM21 Associates with MITRAC Complexes

(A) Mitochondria from MITRAC12^{FLAG}-expressing and control cells were grown on SILAC medium. Equal amounts of mitochondria were pooled, solubilized, and subjected to native complex isolation with anti-FLAG-agarose. Eluted complexes were analyzed by BN-PAGE and western blotting.

(B) Eluates from (A) analyzed by BN-PAGE. Gel lanes were cut into 20 slices (1, top; 20, bottom) followed by LC-MS analysis. Profiles were calculated for significantly enriched proteins from mean intensities, normalized to maximum intensity, and plotted over the 20 slices. Left: MITRAC12 profile. Profiles were

(legend continued on next page)

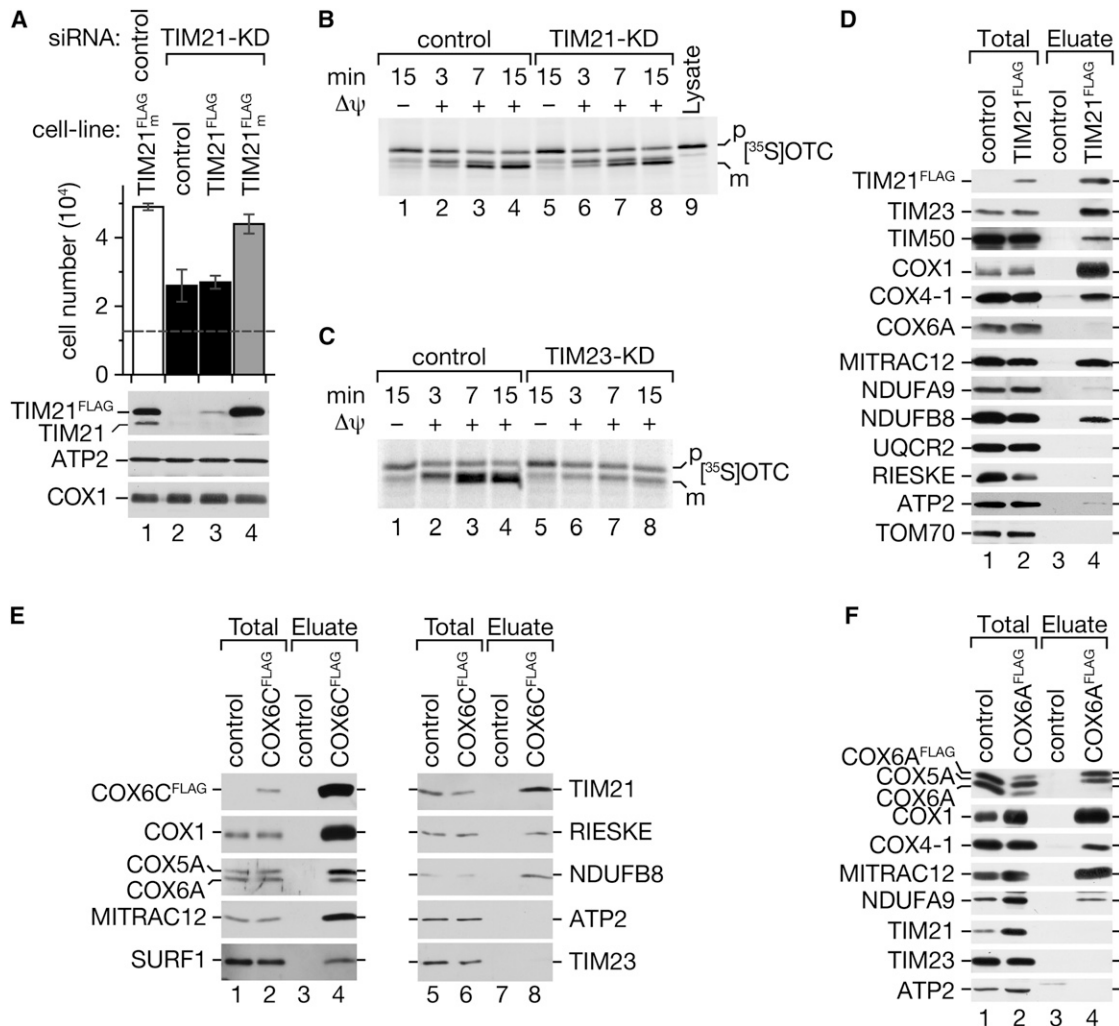


Figure 6. TIM21 Associates with the TIM23 Complex and Complex IV Intermediates

(A) Control cells and cells expressing TIM21^{FLAG} or siRNA-resistant TIM21^{FLAG}_m were transfected with siRNAs against TIM21 or nontargeting control as indicated. Cells were grown for 72 hr, harvested, and counted (top, SEM, n = 3) or analyzed by SDS-PAGE and western blotting (bottom).

(B and C) [³⁵S]OTC precursors were imported into isolated mitochondria from HEK293 cells transfected with indicated siRNAs in the presence or absence of Δψ for indicated times. Samples were proteinase K treated and analyzed by SDS-PAGE and digital autoradiography. p, precursor; m, mature; Lysate, synthesized precursor.

(D–F) Anti-FLAG IPs from indicated mitochondria. Isolated proteins were analyzed by SDS-PAGE and western blotting. Total, 3.3%; Eluate, 100%.

MITRAC complexes (Figure 5D). However, compared to MITRAC12^{FLAG}, TIM21^{FLAG} coisolated an additional complex with apparent migration of 800 kDa but no defined complex at the size of mature cytochrome c oxidase (Figure 7C). The 800 kDa complex was reminiscent of the previously characterized complex I assembly intermediate of 830 kDa containing

mitochondria-encoded subunits as well as nuclear-encoded NDUFB8 (Dunning et al., 2007; Lazarou et al., 2009). To further support that TIM21 was associated with a complex I assembly intermediate, we imported ³⁵S-labeled NDUFB8 and the soluble NDUFS6 and analyzed complexes by BN-PAGE. Whereas [³⁵S] NDUFS6 assembled into mature complex I, [³⁵S]NDUFB8

subjected to hierarchical clustering with Euclidian distances and complete linkage in the R environment (right). Each column represents one protein. Five resulting clusters are indicated. Cluster 2: MITRAC; cluster 3: complex IV; both in red.

(C) Selected profiles from (B). Dashed, intensity peaks of MITRAC12 profile. Gray box, shoulder of early-assembling complex IV subunits.

(D) Complexes isolated from MITRAC12^{FLAG} mitochondria analyzed by SDS-PAGE (left) or 2D-BN/SDS-PAGE (right) and western blotting. Dashed line, MITRAC species containing TIM21.

(E and F) Complexes were purified on anti-FLAG-agarose from mitochondria of indicated HEK293 cells. Samples were analyzed by SDS-PAGE and western blotting.

See also Figure S2 and Table S2.

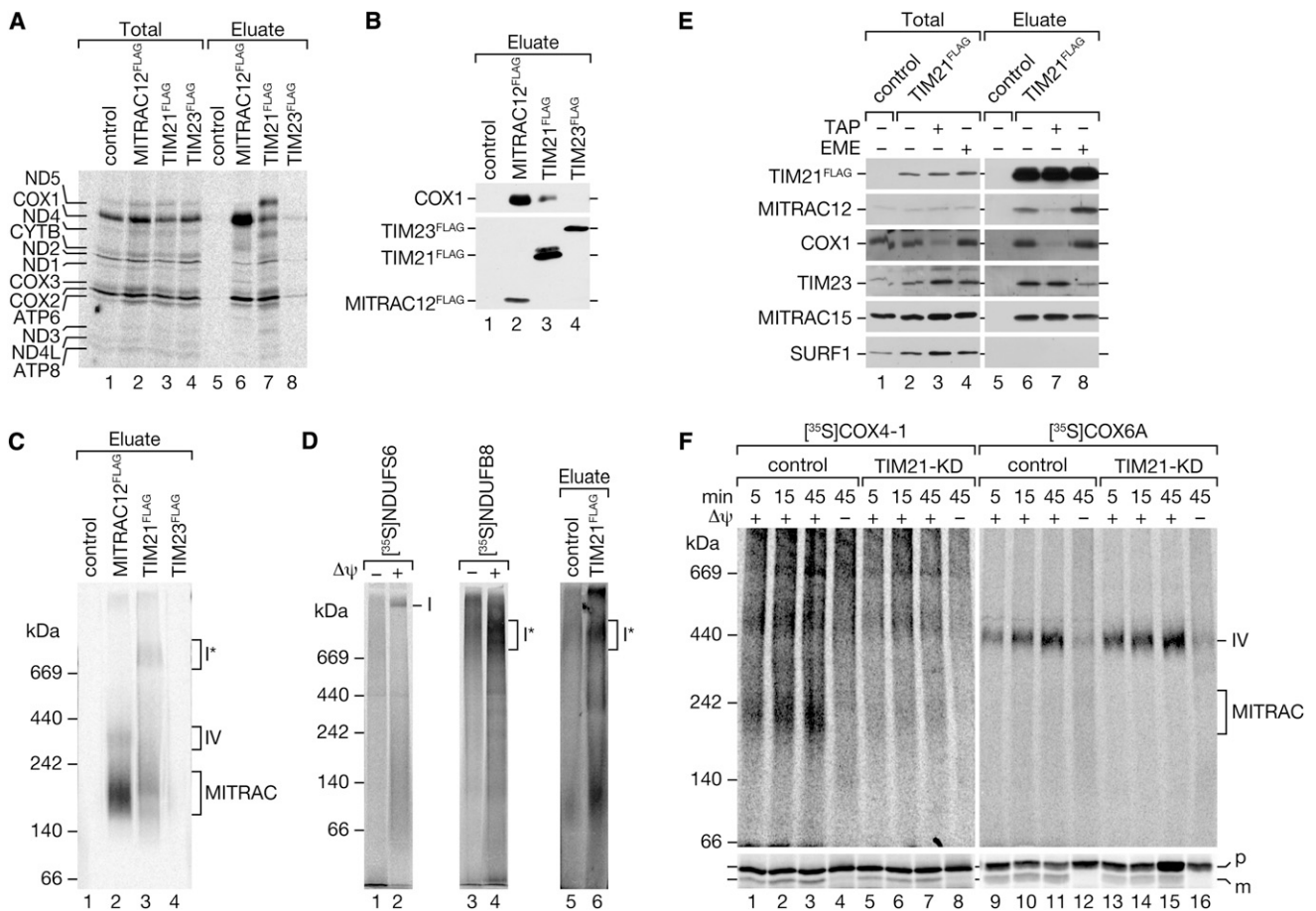


Figure 7. TIM21 Is Required for Assembly of Early Cytochrome c Oxidase Subunits

(A–C) Anti-FLAG IPs from indicated cell lines after radiolabeling of mitochondrial translation products. Samples were separated by SDS- (A and B) or BN-PAGE (C) and analyzed by autoradiography (A and C) or western blotting (B).

(D) [³⁵S]NDUFS6 and [³⁵S]NDUFB8 were imported into HEK293 mitochondria and analyzed by BN-PAGE and autoradiography (lanes 1–4). [³⁵S]NDUFB8 was imported into mitochondria from control or TIM21^{FLAG}-expressing cells. After import, mitochondria were washed, solubilized, and subjected to anti-FLAG IP. Eluates were analyzed by BN-PAGE and autoradiography (lanes 5 and 6). IV, complex IV; I, complex I; I*, complex I assembly intermediate.

(E) Control and TIM21^{FLAG}-expressing cells were treated with thiamphenicol (TAP) or emetine (EME) for 72 and 6 hr, respectively, before anti-FLAG IPs were performed from isolated mitochondria. Samples were analyzed by SDS-PAGE and western blotting. Total, 2%; Eluate, 100%.

(F) Radiolabeled COX4-1 and COX6A were imported into mitochondria from cells transfected with control or TIM21-specific siRNAs. Import reactions were performed for indicated times in the presence or absence of $\Delta\psi$. Samples were split and analyzed by BN-PAGE (upper panel) or SDS-PAGE (lower panel) and digital autoradiography.

See also Figure S2.

formed the reported intermediate (Figure 7D, lanes 1–4). The NDUFB8-containing complex displayed similar apparent migration as the observed TIM21^{FLAG}-purified complex. To investigate a direct association of the 800 kDa NDUFB8-containing complex with TIM21, we imported radiolabeled NDUFB8 into control mitochondria and mitochondria containing TIM21^{FLAG}, which occurred with similar efficiency (Figure S2B). After import, mitochondria were solubilized, and TIM21^{FLAG}-purified complexes analyzed by BN-PAGE. TIM21^{FLAG} specifically enriched the 800 kDa NDUFB8-containing complex as well as two smaller NDUFB8-containing complexes (Figure 7D, lanes 5 and 6). In conclusion, TIM21 associates with complex I assembly intermediates containing mitochondria-encoded and imported subunits.

Because TIM21 interacted with newly synthesized mitochondrial proteins and early-assembling nuclear-encoded subunits, we hypothesized that TIM21 could shuttle between TIM23 and MITRAC complexes to fulfill a more direct function in the assembly process of nuclear-encoded subunits into assembly intermediates. To test this, we blocked synthesis of mitochondria-encoded proteins with thiamphenicol. Under these conditions, the interaction of TIM21 with COX1 and MITRAC12 was strongly reduced without influencing the interaction with TIM23 (Figure 7E). Consistently, blocking cytosolic translation with emetine and concomitantly import of nuclear-encoded subunits reduced the interaction between TIM21 and TIM23, whereas the interaction with COX1 and MITRAC12 remained unaffected

(Figure 7E). Interestingly, the amounts of coisolated MITRAC15 did not change, suggesting that the MITRAC15 interaction with TIM21 was independent of its presence both in assembly intermediates and at the TIM23 complex.

To directly address a function of TIM21 in the transfer of newly imported nuclear-encoded subunits from the TIM23 complex to assembly intermediates, we performed *in vitro* assembly assays of radiolabeled early and late complex IV subunits, COX4-1 and COX6A, respectively. COX6A (Cox13 in yeast) is a peripherally localized subunit of cytochrome *c* oxidase and directly assembles into complex IV, bypassing early assembly intermediates (Vukotic et al., 2012; Lazarou et al., 2009). When radiolabeled COX6A was imported into isolated mitochondria from TIM21-depleted cells, it efficiently assembled into mature complex IV in a membrane-potential-dependent manner, with kinetics similar to those in control mitochondria (Figure 7F). In contrast, the early subunit COX4-1 (Cox5 in yeast) that incorporated into assembly intermediates in control mitochondria failed to assemble in TIM21-depleted mitochondria (Figure 7F). Because the import of COX4-1 was not affected as judged by SDS-PAGE analysis, this result demonstrates a direct involvement of TIM21 in the assembly process of the early-assembling subunit COX4-1.

In summary, these analyses show that in human mitochondria, TIM21 shuttles between the presequence translocase and respiratory-chain assembly intermediates in a process that promotes incorporation of early nuclear-encoded subunits into these complexes.

DISCUSSION

Assembly of respiratory-chain complexes from subunits either translated in mitochondria or imported from the cytosol involves distinct assembly intermediates. Progression of assembly requires complex-specific assembly factors that stabilize the intermediates and promote complex maturation. Accordingly, defects of assembly factors lead to respiratory-chain-complex dysfunction, manifesting itself as mitochondrial encephalomyopathies with frequently observed accumulation of assembly intermediates (Shoubridge, 2001; Smeitink et al., 2006). Although genetic screens revealed a broad range of assembly factors in yeast, human assembly factors and their functions are ill defined. We provide a comprehensive analysis of complex IV assembly factors based on biochemical strategies. These analyses define distinct complex IV assembly intermediates, which we termed MITRAC complexes, consisting of COX1 and nuclear-encoded proteins. Among MITRAC constituents, we identified c12orf62, a protein that was recently shown to be defective in a patient with cytochrome *c* oxidase deficiency (Weraarpachai et al., 2012). Furthermore, the identification of assembly factors, such as CMC1 and COX16, with an undefined function in complex IV assembly or with an established function, such as COX15 and SURF1, both implicated in Leigh Syndrome, supports the specificity of our analyses. Besides identifying components involved, our strategy aimed to provide mechanistic insight into human complex IV assembly. In this regard, two central questions were addressed: (1) How is the supply of the initiator subunit COX1 regulated in human mitochondria?

(2) How do nuclear-encoded subunits engage with assembly intermediates after import and insertion into the inner membrane?

Yeast mitochondria harbor a feedback cycle that links complex IV assembly intermediates to the regulation of COX1 mRNA translation on membrane-bound ribosomes. Inactivation of the mRNA-specific translational activator Mss51 by interaction with Cox1 and the assembly factors Coa1, Coa3, and Cox14 reduces the rate of COX1 translation under conditions of assembly retardation, e.g., a limiting flux of imported subunits (Barrientos et al., 2004; Fontanesi et al., 2011; Mick et al., 2007, 2010; Perez-Martinez et al., 2003; Pierrel et al., 2007). Here we identified the components of the MITRAC complexes in human cells, indicating that coupling of assembly-intermediate formation to COX1 translation has been evolutionarily conserved. However, opposite of the situation in yeast mitochondria, the MITRAC components we investigated positively regulate COX1 translation. Knockdown of MITRAC12, proposed to be an ortholog of Coa3 based on sequence similarity (Szklarczyk et al., 2012), selectively decreases COX1 synthesis. Its early role in COX1 biogenesis provides the molecular basis for a recent analysis of the *D. melanogaster* MITRAC12 homolog, CCDC56, the lack of which led to defective complex IV (Peralta et al., 2012). Human c12orf62, which we also show to be a MITRAC component and which is proposed to be an ortholog of yeast Cox14 (Szklarczyk et al., 2012), was suggested to be a negative regulator of COX1 translation as in yeast (Szklarczyk et al., 2012); however, our analyses here, and the analysis of cells from patients with c12orf62 mutations (Weraarpachai et al., 2012), clearly show that loss of c12orf62 leads to reduced COX1 translation. It is not surprising to find that the coupling of COX1 synthesis to complex IV assembly is different in humans versus yeast as the human COX1 mRNA lacks a significant 5' untranslated region (UTR), which is essential for the regulation mechanism in yeast (Perez-Martinez et al., 2003). However, in agreement with a link between assembly and translational regulation in human mitochondria, a patient with mutated COX3 displayed reduced synthesis of the initiator subunit COX1 (Tiranti et al., 2000). Efficient translation of COX1 in humans also requires the translational activator TACO1, but deletion of the yeast ortholog produces no obvious mitochondrial translation phenotype (Weraarpachai et al., 2009). Despite these differences, we find that COX1 translation is linked to the MITRAC complexes in human mitochondria, possibly providing a means for feedback regulation. The molecular details on how the translation process connects with MITRAC remain to be determined; however, it is tempting to speculate that essential mammalian components exist among the proteins identified here.

During complex IV assembly, imported subunits engage with mitochondria-encoded COX1 in assembly intermediates. Interestingly, the majority of imported complex IV subunits present N-terminal presequences and are transported by the presequence translocase (Vögtle et al., 2009). Our analyses demonstrate that progression of complex IV assembly requires nuclear-encoded subunits to utilize this import pathway: human TIM21 associates with the presequence translocase as well as MITRAC complexes in a dynamic manner. Each association relies on the supply of subunits from either the cytosol or the

mitochondrial matrix, suggesting that human TIM21 ushers nuclear-encoded proteins to assembly intermediates. In agreement with this, assembly of the early cytochrome *c* oxidase subunit COX4-1 requires TIM21, whereas it is dispensable for late-assembling subunits. The finding that TIM21 also interacts with complex I intermediates points to a more general role of TIM21 in respiratory-chain assembly. Furthermore, TIM21 appears to be tightly connected to MITRAC15, which, in contrast to TIM23 and MITRAC12, coimmunoprecipitates with TIM21 under all tested conditions. MITRAC15 associates with MITRAC and is required for complex IV but also complex I assembly. Hence, both proteins apparently represent assembly factors with a more general function for respiratory-chain biogenesis.

Future investigations on TIM21 and MITRAC15 function in MITRAC complexes and potential assembly intermediates of other respiratory-chain complexes will be required to unravel the molecular details of translational regulation of the central mitochondria-encoded subunits in humans and elucidate mechanisms of communication between nuclear and mitochondrial gene expression.

EXPERIMENTAL PROCEDURES

Mass spectrometric analyses, data analyses, cell-culture conditions, generation of cell lines, siRNA constructs and transfections, cell-lysate generation, mitochondrial isolation, and localization analysis are described in the [Extended Experimental Procedures](#).

In Vitro Protein Import into Isolated Mitochondria

Open reading frames encoding mitochondrial precursor proteins were cloned into pGEM4Z (Promega). [³⁵S]-labeled precursor proteins were synthesized in vitro with TNT SP6 Quick Coupled Transcription/Translation system (Promega). Alternatively, RNA was in vitro transcribed and purified (mMESSAGE mMACHINE SP6 Kit, MEGAClear Kit; Ambion) and used for in vitro translation with the Flexi Rabbit Reticulocyte Lysate System (Promega). In vitro import into isolated human mitochondria was performed as described ([Lazarou et al., 2009](#)). Radiolabeled proteins were detected after SDS- or BN-PAGE by exposing gels on Storage Phosphor Screens and digitizing signals with a Storm 820 scanner (GE Healthcare).

In Vivo Labeling of Mitochondrial Translation Products

Labeling was performed as described previously ([Chomyn, 1996](#)). Cytosolic translation was inhibited with 100 μg/ml emetine (Invitrogen), and mitochondrial translation pulsed with 0.2 mCi/ml [³⁵S]methionine for 1 hr. In chase experiments, emetine was replaced by cycloheximide, and cells were labeled for 2 hr and washed two times with warm DMEM followed by 7 hr incubation at 37°C under 5% CO₂ atmosphere. Cells were harvested and either lysed for direct analysis or used for mitochondrial isolations. One hundred micrograms of cells were analyzed by SDS-PAGE, or 200 μg of mitochondrial fraction for BN- or 2D-BN/SDS-PAGE analyses (see [Figure 2I](#)). For pulse-chase analyses ([Figure 2G](#)), anisomycin was used instead of emetine. Cells were labeled for 1 hr when the medium was replaced by standard growth medium. Quantification of digital autoradiography signals was performed with ImageQuant TL software (GE Healthcare). COX1 signals were standardized to ND2 or COX3 depending on their separation from other radiolabeled mitochondrial proteins after SDS-PAGE.

BN-PAGE Analysis

Cells or mitochondria were solubilized in buffer (1% digitonin, 20 mM Tris-HCl, pH 7.4, 0.1 mM EDTA, 50 mM NaCl, 10% (w/v) glycerol, and 1 mM PMSF) to a final concentration of 1 μg/μl (2 μg/μl for 2D-PAGE) for 30–45 min at 4°C. Lysates were cleared by centrifugation (20,000 g, 15 min, 4°C) before addition of 10× loading dye (5% Coomassie brilliant blue G-250, 500 mM 6-aminohex-

anoic acid, and 100 mM Bis-Tris, pH 7.0) and separated on 4%–13% or 4%–14% polyacrylamide gradient gels as described ([Wittig et al., 2006](#)).

Miscellaneous

Standard methods were used for SDS-PAGE and western blotting of proteins to polyvinylidene fluoride membranes (Millipore). Primary antibodies were raised in rabbit or purchased (anti-FLAG and anti-c7orf44, Sigma; anti-ATP2 and UQCRC2, Invitrogen; anti-Prohibitin, Abcam). Antigen-antibody complexes were detected by fluorophore- or HRP-coupled secondary antibodies and laser scanning on an FLA-9000 or enhanced chemiluminescence detection on X-ray films (GE Healthcare). In-gel activity assays were performed according to published procedures ([Wittig et al., 2006](#)).

SUPPLEMENTAL INFORMATION

Supplemental Information includes Extended Experimental Procedures, two figures, and two tables and can be found with this article online at <http://dx.doi.org/10.1016/j.cell.2012.11.053>.

ACKNOWLEDGMENTS

We thank C. Schulz, M. Deckers, and B. Schrul for helpful discussion; J. Melin for critical reading of the manuscript; D. Görlich for his support; and M. Balleininger, M. Wissel, B. Knapp, and K. Lobenwein for technical assistance. This work was supported by the Deutsche Forschungsgemeinschaft, SFB860, Excellence Initiative of the German Federal & State, Governments (EXC 294 BIOS) (B.W.), operating grant from the CIHR (E.A.S.), and the Max-Planck-Society (P.R.). E.A.S. is an HHMI international scholar.

Received: July 27, 2012

Revised: October 10, 2012

Accepted: November 30, 2012

Published: December 20, 2012

REFERENCES

- Barrientos, A., Korr, D., and Tzagoloff, A. (2002). Shy1p is necessary for full expression of mitochondrial COX1 in the yeast model of Leigh's syndrome. *EMBO J.* 21, 43–52.
- Barrientos, A., Zambrano, A., and Tzagoloff, A. (2004). Mss51p and Cox14p jointly regulate mitochondrial Cox1p expression in *Saccharomyces cerevisiae*. *EMBO J.* 23, 3472–3482.
- Carr, H.S., and Winge, D.R. (2003). Assembly of cytochrome *c* oxidase within the mitochondrion. *Acc. Chem. Res.* 36, 309–316.
- Chacinska, A., Koehler, C.M., Milenkovic, D., Lithgow, T., and Pfanner, N. (2009). Importing mitochondrial proteins: machineries and mechanisms. *Cell* 138, 628–644.
- Chomyn, A. (1996). In vivo labeling and analysis of human mitochondrial translation products. *Methods Enzymol.* 264, 197–211.
- Dolezal, P., Likic, V., Tachezy, J., and Lithgow, T. (2006). Evolution of the molecular machines for protein import into mitochondria. *Science* 313, 314–318.
- Dunning, C.J.R., McKenzie, M., Sugiana, C., Lazarou, M., Silke, J., Connelly, A., Fletcher, J.M., Kirby, D.M., Thorburn, D.R., and Ryan, M.T. (2007). Human CIA30 is involved in the early assembly of mitochondrial complex I and mutations in its gene cause disease. *EMBO J.* 26, 3227–3237.
- Fontanesi, F., Clemente, P., and Barrientos, A. (2011). Cox25 teams up with Mss51, Ssc1, and Cox14 to regulate mitochondrial cytochrome *c* oxidase subunit 1 expression and assembly in *Saccharomyces cerevisiae*. *J. Biol. Chem.* 286, 555–566.
- Horn, D., Al-Ali, H., and Barrientos, A. (2008). Cmc1p is a conserved mitochondrial twin CX9C protein involved in cytochrome *c* oxidase biogenesis. *Mol. Cell. Biol.* 28, 4354–4364.

- Khalimonchuk, O., Bird, A., and Winge, D.R. (2007). Evidence for a pro-oxidant intermediate in the assembly of cytochrome oxidase. *J. Biol. Chem.* *282*, 17442–17449.
- Lazarou, M., Smith, S.M., Thorburn, D.R., Ryan, M.T., and McKenzie, M. (2009). Assembly of nuclear DNA-encoded subunits into mitochondrial complex IV, and their preferential integration into supercomplex forms in patient mitochondria. *FEBS J.* *276*, 6701–6713.
- Mashkevich, G., Repetto, B., Glerum, D.M., Jin, C., and Tzagoloff, A. (1997). SHY1, the yeast homolog of the mammalian SURF-1 gene, encodes a mitochondrial protein required for respiration. *J. Biol. Chem.* *272*, 14356–14364.
- Mick, D.U., Wagner, K., van der Laan, M., Frazier, A.E., Perschil, I., Pawlas, M., Meyer, H.E., Warscheid, B., and Rehling, P. (2007). Shy1 couples Cox1 translational regulation to cytochrome c oxidase assembly. *EMBO J.* *26*, 4347–4358.
- Mick, D.U., Vukotic, M., Piechura, H., Meyer, H.E., Warscheid, B., Deckers, M., and Rehling, P. (2010). Coa3 and Cox14 are essential for negative feedback regulation of COX1 translation in mitochondria. *J. Cell Biol.* *191*, 141–154.
- Mick, D.U., Fox, T.D., and Rehling, P. (2011). Inventory control: cytochrome c oxidase assembly regulates mitochondrial translation. *Nat. Rev. Mol. Cell Biol.* *12*, 14–20.
- Neupert, W., and Herrmann, J.M. (2007). Translocation of proteins into mitochondria. *Annu. Rev. Biochem.* *76*, 723–749.
- Peralta, S., Clemente, P., Sánchez-Martínez, A., Calleja, M., Hernández-Sierra, R., Matsushima, Y., Adán, C., Ugalde, C., Fernández-Moreno, M.A., Kaguni, L.S., and Garesse, R. (2012). Coiled coil domain-containing protein 56 (CCDC56) is a novel mitochondrial protein essential for cytochrome c oxidase function. *J. Biol. Chem.* *287*, 24174–24185.
- Perez-Martínez, X., Broadley, S.A., and Fox, T.D. (2003). Mss51p promotes mitochondrial Cox1p synthesis and interacts with newly synthesized Cox1p. *EMBO J.* *22*, 5951–5961.
- Pierrel, F., Bestwick, M.L., Cobine, P.A., Khalimonchuk, O., Cricco, J.A., and Winge, D.R. (2007). Coa1 links the Mss51 post-translational function to Cox1 cofactor insertion in cytochrome c oxidase assembly. *EMBO J.* *26*, 4335–4346.
- Reinhold, R., Bareth, B., Balleininger, M., Wissel, M., Rehling, P., and Mick, D.U. (2011). Mimicking a SURF1 allele reveals uncoupling of cytochrome c oxidase assembly from translational regulation in yeast. *Hum. Mol. Genet.* *20*, 2379–2393.
- Saddar, S., Dienhart, M.K., and Stuart, R.A. (2008). The F₁F₀-ATP synthase complex influences the assembly state of the cytochrome bc₁-cytochrome oxidase supercomplex and its association with the TIM23 machinery. *J. Biol. Chem.* *283*, 6677–6686.
- Shoubridge, E.A. (2001). Cytochrome c oxidase deficiency. *Am. J. Med. Genet.* *106*, 46–52.
- Smeitink, J.A., Zeviani, M., Turnbull, D.M., and Jacobs, H.T. (2006). Mitochondrial medicine: a metabolic perspective on the pathology of oxidative phosphorylation disorders. *Cell Metab.* *3*, 9–13.
- Soto, I.C., Fontanesi, F., Liu, J., and Barrientos, A. (2012). Biogenesis and assembly of eukaryotic cytochrome c oxidase catalytic core. *Biochim. Biophys. Acta* *1817*, 883–897.
- Strogolova, V., Furness, A., Robb-McGrath, M., Garlich, J., and Stuart, R.A. (2012). Rcf1 and Rcf2, members of the hypoxia-induced gene 1 protein family, are critical components of the mitochondrial cytochrome bc₁-cytochrome c oxidase supercomplex. *Mol. Cell Biol.* *32*, 1363–1373.
- Szklarczyk, R., Wanschers, B.F., Cuypers, T.D., Esseling, J.J., Riemersma, M., van den Brand, M.A., Gloerich, J., Lasonder, E., van den Heuvel, L.P., Nijtmans, L.G., and Huynen, M.A. (2012). Iterative orthology prediction uncovers new mitochondrial proteins and identifies C12orf62 as the human ortholog of COX14, a protein involved in the assembly of cytochrome c oxidase. *Genome Biol.* *13*, R12.
- Tiranti, V., Corona, P., Greco, M., Taanman, J.W., Carrara, F., Lamantea, E., Nijtmans, L., Uziel, G., and Zeviani, M. (2000). A novel frameshift mutation of the mtDNA COIII gene leads to impaired assembly of cytochrome c oxidase in a patient affected by Leigh-like syndrome. *Hum. Mol. Genet.* *9*, 2733–2742.
- van der Laan, M., Wiedemann, N., Mick, D.U., Guiard, B., Rehling, P., and Pfanner, N. (2006). A role for Tim21 in membrane-potential-dependent preprotein sorting in mitochondria. *Curr. Biol.* *16*, 2271–2276.
- Vögtle, F.-N., Wortelkamp, S., Zahedi, R.P., Becker, D., Leidhold, C., Gevaert, K., Kellermann, J., Voos, W., Sickmann, A., Pfanner, N., and Meisinger, C. (2009). Global analysis of the mitochondrial N-proteome identifies a processing peptidase critical for protein stability. *Cell* *139*, 428–439.
- Vukotic, M., Oeljeklaus, S., Wiese, S., Vögtle, F.-N., Meisinger, C., Meyer, H.E., Ziesenis, A., Katschinski, D.M., Jans, D.C., Jakobs, S., et al. (2012). Rcf1 mediates cytochrome oxidase assembly and respirasome formation, revealing heterogeneity of the enzyme complex. *Cell Metab.* *15*, 336–347.
- Wagner, K., Rehling, P., Sanjuán Szklarz, L.K., Taylor, R.D., Pfanner, N., and van der Laan, M. (2009). Mitochondrial F₁F₀-ATP synthase: the small subunits e and g associate with monomeric complexes to trigger dimerization. *J. Mol. Biol.* *392*, 855–861.
- Weraarpachai, W., Antonicka, H., Sasarman, F., Seeger, J., Schrank, B., Kolesar, J.E., Lochmüller, H., Chevrette, M., Kaufman, B.A., Horvath, R., and Shoubridge, E.A. (2009). Mutation in TACO1, encoding a translational activator of COX I, results in cytochrome c oxidase deficiency and late-onset Leigh syndrome. *Nat. Genet.* *41*, 833–837.
- Weraarpachai, W., Sasarman, F., Nishimura, T., Antonicka, H., Auré, K., Rötig, A., Lombès, A., and Shoubridge, E.A. (2012). Mutations in C12orf62, a factor that couples COX I synthesis with cytochrome c oxidase assembly, cause fatal neonatal lactic acidosis. *Am. J. Hum. Genet.* *90*, 142–151.
- Wittig, I., Braun, H.-P., and Schägger, H. (2006). Blue native PAGE. *Nat. Protoc.* *1*, 418–428.

EXTENDED EXPERIMENTAL PROCEDURES

Mass Spectrometry

Affinity-purified proteins were separated by gel electrophoresis and stained with colloidal Coomassie Brilliant Blue G-250. The corresponding lanes were cut into individual slices and further processed for in-gel digestion of proteins using trypsin as described previously (Wiese et al., 2007). Tryptic digests were analyzed by LC-MS employing an Ultimate 3000 RSLCnano/LTQ-Orbitrap XL system (Thermo Fisher Scientific, Bremen, Germany) essentially as described previously (Kaller et al., 2011). In brief, peptides were loaded onto one of two C18 μ -pre-columns (Acclaim PepMap μ -Precolumn Cartridge; 0.3 mm \times 5 mm, particle size 5 μ m, Thermo Scientific Dionex) and pre-concentrated for 5 min at a flow rate of 30 μ l/min using solvent A (0.1% (v/v) trifluoroacetic acid [TFA]). The pre-column was switched in line with a C18 RP nano LC column (Acclaim PepMap RSLC analytical column, 75 μ m \times 25 cm, 2 μ m, 100 Å , Thermo Scientific Dionex), and peptides were separated using a linear gradient consisting of 5%–40% solvent B (0.1% (v/v) formic acid [FA] in 84% (v/v) acetonitrile [ACN]) in 30 min and 40%–95% solvent B in 5 min. Subsequently, the analytical column was washed (95% solvent B, 5 min) and equilibrated (5% solvent B, 15 min) applying a flow rate of 300 nl/min. To minimize carry-over, pre-columns were washed with 0.1% (v/v) TFA with increasing concentrations (v/v) of ACN (0% for 5 min, 50% for 20 min and 84% for 15 min) before re-equilibration with 0.1% TFA.

The LTQ-Orbitrap XL was equipped with a nano-electrospray ion source (Thermo Fisher Scientific) using distal coated SilicaTips (FS360-20-10-D, New Objective, Woburn, MA, USA) and weekly calibrated using standard compounds to obtain high mass accuracy. The operation parameters were as follows: spray voltage, 1.5 kV; capillary voltage, 44–45 V; capillary temperature, 200°C; tube lens voltage, 100–120 V. Data-dependent analyses were performed using XCalibur 2.0 SR 2 (Thermo Fisher Scientific). MS survey scans were acquired in the orbitrap (m/z 370 to 1,700; resolution of 60,000 at m/z 400) with an AGC value of 5×10^5 ions and a maximum fill time of 500 ms. A TOP5 method was applied to obtain MS/MS spectra of multiple charged ions by low-energy collision-induced dissociation (CID) in the LTQ (AGC: 10,000 ions, max. fill time: 400 ms). For CID experiments, a normalized collision energy of 35%, an activation q of 0.25 and an activation time of 30 ms were used. The target ion value was set to 2,500 and a dynamic exclusion time of 45 s was placed on previously selected precursor ions.

Mass Spectrometric Data Analysis

MaxQuant (version 1.2.0.18) was used for data processing (Cox and Mann, 2008; Cox et al., 2011). Peak lists were searched against the IPI human database (version 3.68) containing 87,061 protein entries. Peptides and proteins were identified with a false discovery rate of <1% employing the following search criteria: MS tolerance for “first search” 20 ppm, initial MS and MS/MS mass tolerances of 6 ppm and 0.4 Da, respectively; at least one unique peptide (≥ 6 amino acids); trypsin as enzyme with a maximum of two missed cleavages; methionine oxidation and dimethylation at lysine or arginine as variable modification; $^{13}\text{C}_6$ $^{15}\text{N}_2$ -lysine and $^{13}\text{C}_6$ $^{15}\text{N}_4$ -arginine as heavy labeled amino acids. If peptides were assigned to different proteins or multiple isoforms, the respective proteins were reported as a single protein group. For SILAC (stable isotope labeling of amino acids in cell culture)-based quantification of proteins or protein groups, “razor” peptides and a minimum ratio count of two were considered. In addition, “requantify” and “filter labeled amino acids” were enabled and low-scoring peptides were excluded.

For the SILAC-based analysis of MITRAC12 complexes by denaturing gel electrophoresis, the normalized light-over-heavy (L/H; replicates 1 and 3) or heavy-over-light (H/L; replicates 2 and 4) ratios were calculated. Ratios were log-transformed, and the mean \log_{10} ratio across all experiments was calculated for each protein. A one-sided t test was performed to determine p values for all proteins quantified in at least two experiments. Proteins considered to specifically enrich with the bait protein MITRAC12 were required to be identified with at least two peptides as well as quantified with a mean ratio of ≥ 15 and a p value of < 0.01 . The proteins COX16, C12orf62, and CMC1 were requantified in three individual replicates using an in-house built algorithm. Briefly, accurate m/z values of the corresponding peptide pairs were determined and the extracted ion chromatograms (XICs) of the first three isotopic peaks of each SILAC pair were calculated with a mass accuracy of m/z 0.05. In addition, mass spectra were manually inspected to ensure that isotope clusters correspond to peptide identifications. Relative quantification was performed by integration of XICs. For peptides that were only detected in the “complex” and not present in the “control,” the SILAC ratio was set to a value of 100. Raw data and MaxQuant output files can be provided on request.

SILAC data obtained from affinity-purified MITRAC12 complexes separated by BN-PAGE in two individual repeats were subjected to hierarchical clustering performed in the R environment using Euclidian distances and complete linkage. Only proteins reliably identified in both repeats with at least two peptides were considered and common contaminants like keratins were excluded. In addition, proteins were required to be enriched in both repeats with a minimum SILAC ratio of three in at least one replicate. Protein profiles were calculated based on the mean of all peptide intensities assigned to a given protein in each sample (slices 1–20) and normalized to the slice with the highest intensity.

Cell Culture and Generation of Cell Lines

Human embryonic kidney cell lines (HEK293T and Flp-InTM T-REXTM 293) were cultured in DMEM (Dulbecco's Modified Eagle Medium) supplemented with 10% (v/v) fetal bovine serum (FBS) (GIBCO, Invitrogen), 2 mM L-glutamine, and 50 μ g/ml uridine at 37°C under a 5% CO₂ humidified atmosphere. For SILAC experiments, cells were grown for 5 passages on “SILAC” DMEM medium

(lacking arginine and lysine) containing 10% (v/v) dialysed FBS (PAA), with the following modifications: all media were supplemented with 600 mg/l proline, 42 mg/l arginine hydrochloride ($^{13}\text{C}_6^{15}\text{N}_4$ -arginine in “heavy” media), and 146 mg/l lysine hydrochloride ($^{13}\text{C}_6^{15}\text{N}_2$ -lysine in “heavy” media) (EURISO-TOP). The incorporation of heavy amino acids was determined to be 98% and heavy arginine to proline conversion was below 0.5%.

For inhibition of mitochondrial or cytosolic translation the medium was supplemented with 50 $\mu\text{g}/\text{ml}$ thiamphenicol (Sigma-Aldrich) for 3 days or 20 $\mu\text{g}/\text{ml}$ emetine (Sigma-Aldrich) for 6 hr, respectively. Constructs to facilitate inducible expression of C-terminally FLAG-tagged proteins were prepared by amplification of gene specific PCR fragments, using cDNA templates originating from HEK293 cells. Primers were designed based on the appropriate NCBI sequences (MITRAC12 NM_001040431.1, TIM21 NM_014177.2, COX6A NM_005205.3, COX6C NM_004374.3, TIM23 NM_006327.2, CMC1 NM_001179703.1, MITRAC15 NM_018224.3, C12orf62 NM_032901.3) and FLAG peptide sequences were introduced before the stop codons in the reverse primers. Amplicons and pcDNA5/FRT/TO (Invitrogen) were digested with appropriate enzymes, ligated and final constructs confirmed by sequencing. Cell lines expressing the transcript of interest were generated as described previously (Dennerlein et al., 2010).

siRNA Constructs and Transfection

The following sequences and concentrations were applied: TIM21 (5'-CCCAGGAAGUGGUGAAUUAU-3'; 8 nM), TIM23 (5'-CCCUCU GUCUCCUUAUUUA-3', 8 nM), MITRAC12 (5'-CGCAGUUGUUACGAGGUUA-3', 33 nM), and C12orf62 (5'-CCUUCUCUACCUC CAUGAU-3', 33 nM). Reverse transfections were performed as described in Ovcharenko et al. (2005) on approximately 250,000 cells/25 cm^2 with Lipofectamine RNAiMAX (Invitrogen) in OptiMEM-I medium. HEK293 cells were analyzed after 72 hr of knockdown and fibroblasts after 9 days (Weraarpachai et al., 2012). In the case of Figures 2C and 2D, cells were retransfected after 48 hr.

Cell Lysates, Mitochondrial Isolation, and Localization Analysis

Whole-cell lysates were prepared as described (Dennerlein et al., 2010) and mitochondria isolated by differential centrifugation (Lazarou et al., 2009). Protein concentrations were determined by Bradford analysis using bovine serum albumin (BSA) as a standard. Membrane integration of proteins was analyzed by incubation of mitochondria in 100 mM Na_2CO_3 (pH 11.5). Subsequently, integral membrane proteins were sedimented with membranes (45 min 45,000 \times g 4°C). Submitochondrial localization was analyzed by protease protection assay: mitochondrial membranes were osmotically stabilized in SEM buffer (250 mM sucrose, 1 mM EDTA, and 10 mM MOPS, pH 7.2), outer mitochondrial membrane ruptured by EM buffer (1 mM EDTA and 10 mM MOPS, pH 7.2), or mitochondrial membranes disrupted by sonication in the presence of proteinase K. After incubation for 10 min on ice, reactions were stopped by addition of 1 mM PMSF. Samples were precipitated with trichloroacetic acid.

Cytochrome c Oxidase Activity and Quantitation Assay

The specific activity and relative amount of cytochrome c oxidase were measured by using Complex IV Human Specific Activity Microplate Assay Kit from Mitosciences (Abcam) according to the manufacturer's instructions. In brief, cells were harvested, homogenized, and solubilized. Twenty micrograms of total protein were loaded in each well of the plate. Cytochrome c oxidase activity was determined by measuring the oxidization of cytochrome c and the consequent change of absorbance at 550 nm. The relative amount of cytochrome c oxidase was determined measuring the increase of absorbance at 405 nm after the incubation with a specific antibody for complex IV conjugated to alkaline phosphatase. The measurements were performed in a BioTek Synergy H4 Hybrid Multi-Mode plate reader.

Affinity Purification Procedures

Isolated mitochondria harboring affinity-tagged proteins or control mitochondria were solubilized in buffer (20 mM Tris-HCl, pH 7.4, 100 mM NaCl, 0.5 mM EDTA, 10% (w/v) glycerol, and 1 mM phenylmethylsulfonyl fluoride [PMSF]) containing 1% (w/v) digitonin (Merck) to a final concentration of 1 μg protein/ μl and incubated for 30 min at 4°C under mild agitation. Lysate was cleared by centrifugation (20,000 \times g, 15 min, 4°C). Supernatants were applied to equilibrated affinity resins: anti-FLAG-agarose (Sigma), IgG-sepharose or ProteinA-sepharose (GE Healthcare) conjugated with anti-MITRAC12 or control antibodies. After incubation at 4°C for 60–90 min under mild agitation, unbound material was collected, and affinity resins washed extensively with buffer containing 0.3% digitonin. Bound proteins were eluted depending on affinity resins used: Proteins bound to anti-MITRAC12 and control resins were eluted with 0.1 M glycine (pH 2.8), SURF1^{ZZ} and bound proteins were eluted by an overnight tobacco etch virus protease treatment at 4°C, and proteins isolated by anti-FLAG-agarose were eluted with 5 $\mu\text{g}/\text{ml}$ FLAG peptide in wash buffer. Standard experiments were performed using 0.5–2 mg isolated mitochondria. For AP/MS experiments, 15 mg of mitochondria were used for SURF1^{ZZ} isolation and 12 mg mixed mitochondria (6 mg per cell line) for anti-FLAG affinity purification for each experiment after SILAC.

SUPPLEMENTAL REFERENCES

Cox, J., and Mann, M. (2008). MaxQuant enables high peptide identification rates, individualized p.p.b.-range mass accuracies and proteome-wide protein quantification. *Nat. Biotechnol.* 26, 1367–1372.

- Cox, J., Neuhauser, N., Michalski, A., Scheltema, R.A., Olsen, J.V., and Mann, M. (2011). Andromeda: a peptide search engine integrated into the MaxQuant environment. *J. Proteome Res.* *10*, 1794–1805.
- Dennerlein, S., Rozanska, A., Wydro, M., Chrzanowska-Lightowlers, Z.M.A., and Lightowlers, R.N. (2010). Human ERAL1 is a mitochondrial RNA chaperone involved in the assembly of the 28S small mitochondrial ribosomal subunit. *Biochem. J.* *430*, 551–558.
- Kaller, M., Liffers, S.-T., Oeljeklaus, S., Kuhlmann, K., Röh, S., Hoffmann, R., Warscheid, B., and Hermeking, H. (2011). Genome-wide characterization of miR-34a induced changes in protein and mRNA expression by a combined pulsed SILAC and microarray analysis. *Mol. Cell. Proteomics* *10*, M111, 010462.
- Lazarou, M., Smith, S.M., Thorburn, D.R., Ryan, M.T., and McKenzie, M. (2009). Assembly of nuclear DNA-encoded subunits into mitochondrial complex IV, and their preferential integration into supercomplex forms in patient mitochondria. *FEBS J.* *276*, 6701–6713.
- Ovcharenko, D., Jarvis, R., Hunicke-Smith, S., Kelnar, K., and Brown, D. (2005). High-throughput RNAi screening in vitro: from cell lines to primary cells. *RNA* *11*, 985–993.
- Weraarpachai, W., Sasarman, F., Nishimura, T., Antonicka, H., Auré, K., Rötig, A., Lombès, A., and Shoubridge, E.A. (2012). Mutations in C12orf62, a factor that couples COX I synthesis with cytochrome c oxidase assembly, cause fatal neonatal lactic acidosis. *Am. J. Hum. Genet.* *90*, 142–151.
- Wiese, S., Gronemeyer, T., Ofman, R., Kunze, M., Grou, C.P., Almeida, J.A., Eisenacher, M., Stephan, C., Hayen, H., Schollenberger, L., et al. (2007). Proteomics characterization of mouse kidney peroxisomes by tandem mass spectrometry and protein correlation profiling. *Mol. Cell. Proteomics* *6*, 2045–2057.

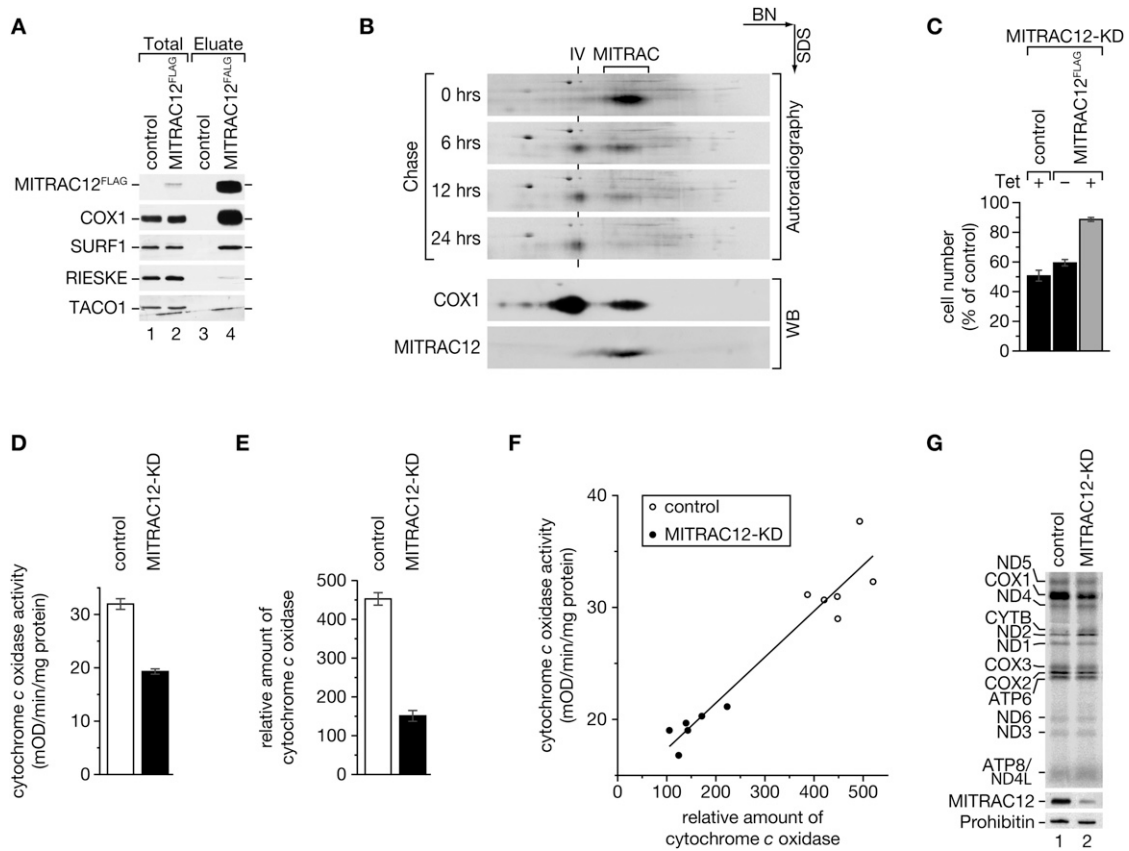


Figure S1. MITRAC Complexes Are Productive Cytochrome c Oxidase Assembly Intermediates that Regulate COX1 Expression, Related to Figure 2

(A) IP from control or MITRAC12^{FLAG}-expressing mitochondria using anti-FLAG-agarose. Bound proteins eluted by FLAG peptide. Total, 2%; Eluate, 100%.

(B) Pulse-Chase analysis of mitochondrial translation products. Mitochondrial translation products have been radiolabeled for 60 min. After removing the labeling medium, cells were supplemented with regular growth medium containing excess amounts of unlabeled methionine. After indicated times, cells were harvested, and mitochondria isolated and analyzed by 2D-BN/SDS-PAGE and autoradiography. As western blotting control (WB), 0 hr chase samples were analyzed. Sections of interest have been excised to visualize the molecular weight range of COX1 in the autoradiographs. IV, mature complex IV.

(C) HEK293 control cells and cells containing MITRAC12^{FLAG} under tetracycline-inducible promoter were transfected with siRNAs against MITRAC12 and treated with tetracycline (Tet) to induce protein expression. Cells were grown for 72 hr, harvested, counted, and normalized to cells transfected with nontargeting control siRNA (SEM, n = 3).

(D–F) Measurement of the activity and relative amount of the cytochrome c oxidase. (D) Cytochrome c oxidase complexes from similar protein amounts were captured by anti-complex IV antibody, and the specific activity of these complexes was measured photometrically (SEM, n = 6). (E) The amount of captured cytochrome c oxidase was measured photometrically using specific alkaline phosphatase-conjugated complex IV antibodies (SEM, n = 6). These measurements (D and E) were determined in quadruplicate from cells incubated in the presence of siRNA directed against MITRAC12 or control siRNA in six independent experiments. (F) The regression plot of activity values and the relative amount of the cytochrome c oxidase shows a strong correlation ($r = 0.96$).

(G) Mitochondrial translation products were radiolabeled in fibroblasts after siRNA treatment against indicated mRNAs. Cells were harvested, lysed, and subjected to SDS-PAGE and autoradiography (top) or western blotting using indicated antibodies (bottom).

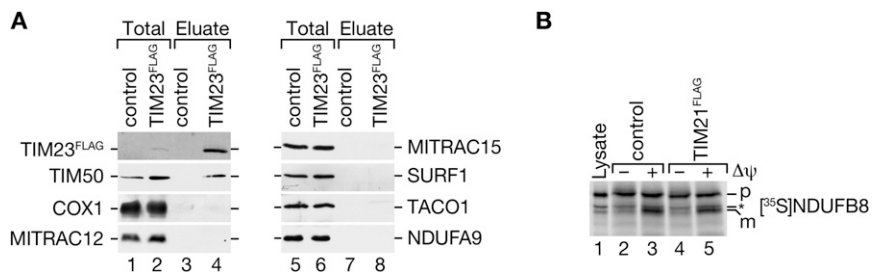


Figure S2. TIM21 Partitions from the Presequence Translocase to Interact with Early Intermediates of Respiratory-Chain Complexes, Related to Figures 5 and 7

(A) Complexes from TIM23^{FLAG} and control mitochondria were isolated via anti-FLAG chromatography and analyzed by SDS-PAGE and western blotting. Total, 2%; Eluate, 100%.

(B) [³⁵S]NDUFB8 precursors were imported into mitochondria from HEK293 cells or corresponding cells expressing TIM21^{FLAG} in the presence or absence of a $\Delta\psi$ for 45 min. Reactions were stopped by dissipating the $\Delta\psi$. Samples were analyzed by SDS-PAGE and digital autoradiography. p, precursor; m, mature; *, unspecific protein band present in the lysate; Lysate, synthesized precursor as comparison.